

1 **Biogenic and anthropogenic sources of isoprene and monoterpenes and their secondary organic**
2 **aerosol in Delhi, India**

3 Daniel J. Bryant¹, Beth S. Nelson¹, Stefan J. Swift^{1a}, Sri Hapsari Budisulistiorini¹, Will S. Drysdale^{1,2},
4 Adam R. Vaughan¹, Mike J. Newland^{1b}, James R. Hopkins^{1,2}, James M. Cash^{3,4}, Ben Langford³, Eiko
5 Nemitz³, W. Joe F. Acton^{5c}, C. Nicholas Hewitt⁵, Tuhin Mandal⁶, Bhola R. Gurjar⁶, Shivani^{6d}, Ranu
6 Gadi⁶, James D. Lee^{1,2}, Andrew R. Rickard^{1,2}, Jacqueline F. Hamilton¹

7 1- Wolfson Atmospheric Chemistry Laboratories, Department of Chemistry, University of York,
8 Heslington, York, YO10 5DD, UK

9 2- National Centre for Atmospheric Science, University of York, Heslington, York, YO10 5DD, UK

10 3- UK Centre for Ecology and Hydrology, Penicuik, Midlothian, Edinburgh, EH26 0QB, UK

11 4- School of Chemistry, University of Edinburgh, Edinburgh, EH9 3FJ, Edinburgh, UK

12 5- Lancaster Environment Centre, Lancaster University, Lancaster, LA1 4YW, UK

13 6- Department of Applied Sciences and Humanities, Indira Gandhi Delhi Technical University for
14 Women, Delhi, 110006, India

15 ^a now at: J. Heyrovsky Institute of Physical Chemistry, Department of Chemistry of Ions in Gaseous
16 Phase, Prague, Czech Republic

17 ^b now at: ICARE-CNRS, 1 C Av. de la Recherche Scientifique, 45071 Orléans CEDEX 2, France

18 ^c now at: School of Geography, Earth and Environmental Sciences, University of Birmingham,
19 Birmingham, B15 2TT, UK

20 ^d now at: Department of Chemistry, Miranda House, Delhi University, Delhi, 110007, India

21 Correspondence email: daniel.bryant@york.ac.uk

22 **Abstract**

23 Isoprene and monoterpenes emissions to the atmosphere are generally dominated by biogenic
24 sources. The oxidation of these compounds can lead to the production of secondary organic aerosol,
25 however the impact of this chemistry in polluted urban settings has been poorly studied. Isoprene
26 and monoterpenes can form SOA heterogeneously via anthropogenic-biogenic interactions resulting
27 in the formation of organosulfates (OS) and nitrooxy-organosulfates (NOS). Delhi, India is one of the
28 most polluted cities in the world, but little is known about the emissions of biogenic VOCs or the
29 sources of SOA. As part of the DELHI-FLUX project, gas phase mixing ratios of isoprene and speciated
30 monoterpenes were measured during pre- and post-monsoon measurement campaigns in central
31 Delhi. Nocturnal mixing ratios of the VOCs were substantially higher during the post-monsoon
32 (isoprene: (0.65 ± 0.43) ppbv, limonene: (0.59 ± 0.11) ppbv, α -pinene: (0.13 ± 0.12) ppbv) than the
33 pre-monsoon (isoprene: (0.13 ± 0.18) ppbv, limonene: 0.011 ± 0.025 (ppbv), α -pinene: $0.033 \pm$
34 0.009) period. At night, isoprene and monoterpene concentrations correlated strongly with CO
35 across during the post-monsoon period. ~~This is one of the first observations in Asia, suggesting~~
36 ~~monoterpene emissions are dominated by anthropogenic sources.~~ Filter samples of particulate
37 matter less than 2.5 microns in diameter ($PM_{2.5}$) were collected and the OS and NOS content
38 analysed using ultrahigh-performance liquid chromatography tandem mass spectrometry (UHPLC-
39 MS²). Inorganic sulfate was shown to facilitate the formation of isoprene OS species across both
40 campaigns. Sulfate contained within OS and NOS species were shown to contribute significantly to

41 the sulfate signal measured via AMS. Strong nocturnal enhancements of NOS species were observed
42 across both campaigns. The total concentration of OS/NOS species contributed an average of $(2.0 \pm$
43 $0.9)$ % and (1.8 ± 1.4) % to the total oxidised organic aerosol, and up to a maximum of 4.2 % and 6.6
44 % across the pre- and post-monsoon periods, respectively. Overall, this study provides the first
45 molecular level measurements of SOA derived from isoprene and monoterpene in Delhi and
46 demonstrates that both biogenic and anthropogenic sources of these compounds can be important
47 in urban areas.

48 1. Introduction

49 India is undergoing significant urbanization and industrialisation, with a rapidly increasing
50 population. According to the WHO, India was home to 9 out of the top 10 most polluted cities in the
51 world in 2020 in terms of annual mean $PM_{2.5}$ (particulate matter less than 2.5 micrometres in
52 diameter) concentrations (WHO, 2018). In Delhi, the population-weighted mean $PM_{2.5}$ was estimated
53 to be 209 (range: 120 – 339.5) $\mu g m^{-3}$ in 2017, over 40 times the WHO annual mean guidelines of 5
54 $\mu g m^{-3}$, and greater than five times India's own standard of 40 $\mu g m^{-3}$ (Balakrishnan et al., 2019). Air
55 pollution is estimated to cause over 1 million deaths per year in India alone (Landrigan et al., 2018).

56 Numerous studies have investigated $PM_{2.5}$ concentrations, characteristics and meteorological effects
57 in Delhi (Anand et al., 2019; Bhandari et al., 2020; Chowdhury et al., 2004; Hama et al., 2020;
58 Kanawade et al., 2020; Miyazaki et al., 2009; Nagar et al., 2017). The key sources of $PM_{2.5}$ identified
59 are secondary aerosol, fossil fuel combustion, municipal waste and biomass burning (Chowdhury et
60 al., 2004; Sharma and Mandal, 2017; Stewart et al., 2021b, 2021a). Previous studies have also shown
61 that alongside extremely high emissions of pollutants, regional sources and meteorology in
62 particular play an important role in high pollution events in Delhi (Bhandari et al., 2020; Sawlani et
63 al., 2019; Schnell et al., 2018; Sinha et al., 2014).

64 Secondary species have been shown to be significant contributors to PM_1 and $PM_{2.5}$ mass in Delhi,
65 with organics contributing 40-70 % of PM_1 mass. (Gani et al., 2019; Shivani et al., 2019; Reyes-
66 Villegas et al., 2021; Sharma and Mandal, 2017) However, limited molecular level analysis of organic
67 aerosol (OA) has been undertaken (Chowdhury et al., 2004; Elzein et al., 2020; Miyazaki et al., 2009;
68 Singh et al., 2021, 2012; Yadav et al., 2021). Kirillova et al., (2014) analysed the sources of water-
69 soluble organic carbon (WSOC) in Delhi, using radiocarbon measurement constraints. The study
70 identified that 79 % of WSOC was classified as non-fossil carbon, attributed to biogenic/biomass
71 burning sources in urban Delhi (Kirillova et al., 2014), similar to other studies from India (Kirillova et
72 al., 2013; Sheesley et al., 2012). Studies across Asia, Europe and North America have also shown high
73 contributions from non-fossil sources to ambient PM concentrations in urban environments (Du et
74 al., 2014; Kirillova et al., 2010; Szidat et al., 2004; Wozniak et al., 2012). The sources of this modern
75 carbon in urban areas are poorly understood, although biomass burning is a key component (Elser et
76 al., 2016; Hu et al., 2016; Lanz et al., 2010; Nagar et al., 2017). Recently in Delhi, solid-fuel
77 combustion sources such as cow dung cake or municipal solid waste have been shown to release
78 over 1000 different organic components into the aerosol phase at emission (Stewart et al., 2021a).
79 Alongside biomass burning, one potential source of this non-fossil aerosol is biogenic secondary
80 organic aerosol (BSOA), which is formed via the oxidation of biogenic volatile organic compounds
81 (BVOCs) and subsequent gas-particle phase transfer (Hallquist et al., 2009; Hoffmann et al., 1997).

82 Isoprene is the most abundant BVOC, with annual global emissions estimates of between 350 - 800
83 $Tg yr^{-1}$ (Guenther et al., 2012; Sindelarova et al., 2014). Globally, isoprene is predominately emitted
84 from biogenic sources, but anthropogenic sources become increasingly important in urban areas
85 especially at night (Borbon et al., 2001; Hsieh et al., 2017; Khan et al., 2018a; Mishra and Sinha,

86 2020; Sahu et al., 2017; Sahu and Saxena, 2015). Monoterpenes are another important BSOA
87 precursor, with annual global emissions estimates of between 89 and 177 Tg yr⁻¹ (Guenther et al.,
88 2012; Sindelarova et al., 2014). Monoterpenes while mainly biogenic, are also emitted from
89 anthropogenic sources such as biomass burning, cooking and fragranced consumer products (Cheng
90 et al., 2018; Gkatzelis et al., 2021; Panopoulou et al., 2020, 2021; Stewart et al., 2021b, 2021c; Zhang
91 et al., 2020).

92 Numerous studies have identified and quantified molecular level markers from isoprene and
93 monoterpenes, especially in the Southeastern-US and China (Brüggemann et al., 2019; Bryant et al.,
94 2020, 2021; Hettiyadura et al., 2019; Huang et al., 2016; Rattanavara et al., 2016b; Wang et al.,
95 2016, 2018a; Yee et al., 2020). The complex sources of isoprene and monoterpenes in highly
96 polluted urban areas make source identification difficult. As such, the SOA markers in this study will
97 be referred to as originating from isoprene or monoterpenes, but the emissions are likely from a
98 mixture of biogenic and anthropogenic sources as discussed previously. (Cash et al., 2021b; Nelson
99 et al., 2021)

100 Recent studies have started to focus on anthropogenic-biogenic interactions, whereby
101 anthropogenic pollutants such as NO_x and sulfate enhance the formation of biogenically derived SOA
102 species. Increased NO or NO₂ concentrations can lead to higher organonitrate (ON) or nitrooxy-
103 organosulfate (NOS) concentrations through RO₂ + NO or VOC + NO₃ pathways. (Morales et al., 2021;
104 Takeuchi and Ng, 2019) Inorganic sulfate formed from the oxidation of SO₂ plays a pivotal role in OS
105 and NOS formation (Bryant et al., 2020; Budisulistiorini et al., 2015; Glasius et al., 2018; Hettiyadura
106 et al., 2019; Hoyle et al., 2011; Xu et al., 2015). Sulfate allows the acid-catalysed uptake of gas phase
107 oxidation products into the particle phase. Both chamber and ambient studies have shown the direct
108 link between sulfate and OS concentrations (Brüggemann et al., 2020a; Bryant et al., 2020;
109 Budisulistiorini et al., 2015; Gaston et al., 2014; Lin et al., 2012; Riva et al., 2019; Surratt et al.,
110 2008a; Xu et al., 2015). Yee et al., (2020) highlighted markers from both the high/low-NO isoprene
111 oxidation pathways correlated linearly with sulfate over a large range of sulfate concentrations (0.01
112 – 10 µg m⁻³) across central Amazonia during the wet and dry seasons and in the SE-US summer. They
113 conclude that the majority of isoprene oxidation products in pre-industrial settings are still expected
114 to be in the form of isoprene OS (OSi), suggesting that they cannot be thought of as purely a
115 biogenic-anthropogenic product (Yee et al., 2020).

116 In this study, offline PM_{2.5} filter samples were collected across two campaigns (pre and post-
117 monsoon) in central Delhi, alongside a comprehensive suite of gas and aerosol atmospheric
118 pollutant measurements. Filters were analysed using ultra-high performance liquid chromatography
119 tandem mass spectrometry and isoprene and monoterpene OS/NOS markers identified and
120 quantified. Isoprene and monoterpene emissions were observed to correlate strongly to
121 anthropogenic markers, suggesting a mixed anthropogenic/biogenic sources of these VOCs. OSi
122 species showed strong seasonality and strong correlations to particulate sulfate. NOS species
123 showed strong nocturnal enhancements, likely due to nitrate radical chemistry. This study is the first
124 molecular level particle phase analysis of OS and NOS markers from isoprene and monoterpenes in
125 Delhi and aims to improve our understanding of the sources of isoprene and monoterpene SOA
126 markers and their formation pathways in extremely polluted urban environments.

127 **2. Experimental**

128 **2.1 Filter collection and site information**

129 PM_{2.5} filter samples were collected as part of the Air Pollution and Human Health (APHH)-India
130 campaign, at the Indira Gandhi Delhi Technical University for Women in New Delhi, India, (28°39'55"
131 N 77°13'56" E). The site is situated inside the third ring road which caters to huge volumes of traffic,
132 with a major road to the east, between the site and the Yamuna River. Two train stations are located
133 to the south and southwest of the site, and there are several green spaces locally in all
134 directions. (Nelson et al., 2021; Stewart et al., 2021c) Filters were collected during two field
135 campaigns in 2018. The first campaign was during the pre-monsoon period, with 35 filters were
136 collected between 28/05/2018 and 05/06/2018. The second campaign during the post-monsoon
137 period, 108 filters were collected between 09/10/2018 and 6/11/2018. Quartz filters (Whatman
138 QMA, 10" by 8") were pre-baked at 550 °C for 5 hours and wrapped in foil before use. Samples were
139 collected using an HiVol sampler (Ecotech 3000, Victoria Australia) with selective PM_{2.5} inlet at a flow
140 rate of 1.33 m³ min⁻¹. Once collected, filters were stored in foil at -20 °C before, during and after
141 transport for UK based analysis.

142 **2.2 Filter extraction**

143 Using a standard square filter cutter, a section of filter was taken with an area of 30.25 cm² which
144 was then cut into roughly 1 cm² pieces and placed in a 20 mL glass vial. Next, 8 mL of LC-MS grade
145 methanol (MeOH, Optima, Fisher Chemical, USA) was added to the sample and sonicated for 45 min.
146 Ice packs were used to keep the bath temperature below room temperature, with the water
147 swapped mid-way through. Using a 5 mL plastic syringe, the MeOH extract was then pushed through
148 a 0.22 µm filter (Millipore) into another sample vial. An additional 2 mL (2 x 1 mL) of MeOH was
149 added to the filter sample, and then extracted through the filter to give a combined extract ~ 10mL.
150 This extract was then reduced to dryness using a Genevac solvent evaporator under vacuum. The dry
151 sample was then reconstituted in 50:50 MeOH:H₂O (Optima, Fisher Chemical, USA) for analysis
152 (Bryant et al., 2020; Spolnik et al., 2018). Extraction efficiencies of 2-methyl-glyceric acid (2-MG-OS)
153 and camphorsulfonic acid were determined using authentic standards spiked onto a pre-baked clean
154 filter and recoveries were calculated to be 71 % and 99 % respectively.

155 **2.3 Ultra-high performance liquid chromatography tandem mass spectrometry (UHPLC-MS²)**

156 The extracted fractions of the filter samples were analysed using an Ultimate 3000 UHPLC (Thermo
157 Scientific, USA) coupled to a Q-Exactive Orbitrap MS (Thermo Fisher Scientific, USA) using data
158 dependent tandem mass spectrometry (ddMS²) with heated electrospray ionization source (HESI).
159 The UHPLC method uses a reversed-phase 5 µm, 4.6 mm × 100 mm, polar end capped Accucore
160 column (Thermo Scientific, UK) held at 40 °C. The mobile phase consisted of water (A, optima grade)
161 and methanol (B, optima grade) both with 0.1 % (v/v) of formic acid (98 % purity, Acros Organics).
162 Gradient elution was used, starting at 90 % (A) with a 1-minute post-injection hold, decreasing to 10
163 % (A) at 26 minutes, returning to the starting mobile phase conditions at 28 minutes, followed by a
164 2-minute hold allowing the re-equilibration of the column. The flow rate was set to 0.3 mL min⁻¹. A
165 sample injection volume of 4 µL was used. The capillary and auxiliary gas heater temperatures were
166 set to 320 °C, with a sheath gas flow rate of 45 (arb.) and an auxiliary gas flow rate of 20 (arb.).
167 Spectra were acquired in the negative ionization mode with a scan range of mass-to-charge (*m/z*) 50
168 to 750, [with a mass resolution of 140,000](#). Tandem mass spectrometry was performed using higher-
169 energy collision dissociation with a stepped normalized collision energy of 10,45 and 60. The
170 isolation window was set to *m/z* 2.0 with a loop count of 10, selecting the 10 most abundant species
171 for fragmentation in each scan.

172 A mass spectral library was built using the compound database function in Tracefinder 4.1 General
173 Quan software (Thermo Fisher Scientific, USA). To build the library, compounds from previous

174 studies (Chan et al., 2010; Nestorowicz et al., 2018; Ng et al., 2008; Riva et al., 2016b; Schindelka et
175 al., 2013; Surratt et al., 2008a) were searched for in an afternoon and a night-time filter sample
176 extract analysis using the Xcalibur software. Further details can be found in Bryant et al., 2021 and
177 the SI. Isoprene ~~and monoterpene-OS~~ and NOS markers were quantified using [authentic standards of](#)
178 [2-MG-OS and 2-methyl tetrol OS \(2-MT-OS\) with later eluting monoterpene OS and NOS quantified](#)
179 [using camphorsulfonic acid. Standards were run across a 9-point calibration curve \(2 ppm – 7.8ppb,](#)
180 [R² > 0.99\)](#) More details about the method [can be found](#) in Bryant et al., 2021. Overall uncertainties
181 associated with calibrations, proxy standards and matrix effects were estimated. The uncertainties
182 associated with 2-MG-OS and ~~2-methyl tetrol OS (2-MT-OS)~~ were calculated to be 58.9 % and 37.6 %
183 respectively, mainly due to the large uncertainties in the matrix correction factors. Isoprene SOA
184 markers quantified by the average of 2-MT-OS and 2-MG-OS calibrations have an associated
185 uncertainty of 69.9 %. For monoterpene SOA species which were quantified by camphorsulfonic
186 acid, the associated uncertainty is estimated to be 24.8 %.

187

188 2.4 Supplementary measurements

189 A suite of complementary measurements were made alongside the filter collection including
190 VOCs (Stewart et al., 2021c), oxygenated-VOCs, NO_x, CO, O₃, SO₂, HONO, photolysis rates and
191 measurements of PM₁ non-refractory aerosol chemical components with a high resolution Aerosol
192 Mass Spectrometer (HR-AMS). Detailed instrument descriptions can be found in Nelson et al.,
193 (2021). Briefly, VOCs and oxygenated-VOCs were measured via two gas-chromatography (GC)
194 instruments (DC-GS-FID and GC-GC-FID). NO_x was measured via a dual channel chemiluminescence
195 analyser with fitted with a blue light converter for NO₂ (Air Quality Designs Inc., Colorado) alongside
196 CO which was measured with a resonance fluorescent instrument (Model AI5002, Aerolaser GmbH,
197 Germany). O₃ was measured as outlined by Squires et al., (2020) using an ozone analyser (49i,
198 Thermo Scientific). SO₂ was measured using a 43i SO₂ analyser (Thermo scientific). High-resolution
199 aerosol mass spectrometry measurements were conducted as outlined in Cash et al., (2021). Ion
200 chromatography measurements were undertaken by the experimental approach outlined by Xu et
201 al., (2020) as part of an intercomparison study. Briefly, filter cuttings were taken from the filter and
202 extracted ultrasonically for 30 mins in 10 mL of ultrapure water and then filtered before analysis (Xu
203 et al., 2020).

204 Meteorology data was downloaded from the NOAA Integrated Surface Database via the Worldmet R
205 package for the Indira Gandhi International Airport (code: 421810-99999) (Carslaw, D., accessed:
206 2021). The planetary boundary layer height (PBLH) was obtained from the ERA5 (ECMWF ReAnalysis
207 5) data product at 0.25° resolution in 1-hour time steps at the position Lat 28.625°, Lon. 77.25°. The
208 data for both campaigns was then selected between the start time of the first filter of that
209 campaign, and the end time of the last filter of the same campaign.

210 3. Results

211 3.1 Meteorology

212 The time series for temperature, RH, planetary boundary layer height (PBLH) and ventilation
213 coefficient (VC) across the pre- and post-monsoon campaigns are shown in Figure S1. For the pre-
214 monsoon campaign, the average air temperature was (35.8 ± 4.5) °C compared to (24.7 ± 4.6) °C in
215 the post-monsoon campaign (Table S2). The pre-monsoon campaign also showed higher average
216 wind speeds, with an average of (3.8 ± 1.4) ms⁻¹, compared to (1.7 ± 1.3) ms⁻¹ in the post-monsoon
217 campaign. The average RH of the pre- and post-monsoon were (39.4 ± 13.6) % and (57.3 ± 16.6) %

Formatted: Superscript

218 respectively, both showing similar diurnals with a minimum around mid-morning and nocturnal
219 maximum (Figure S2). The PBLH shows a similar diurnal between the two campaigns, with the
220 nocturnal boundary layer breaking down around 06:00-07:00 with a midday peak, before re-
221 establishing the nocturnal boundary layer around 19:00. The pre-monsoon PBLH has an average
222 maximum of ~2400 m compared to post-monsoon ~1700 m and a minimum of 270 m compared to
223 52 m (Figure S2). The ventilation coefficient (VC = wind speed x PBLH) has been used previously to
224 identify periods of adverse meteorological conditions and gives an idea of how stagnant atmospheric
225 conditions are and the general role of the atmosphere in the dilution of species. (Gani et al., 2019)
226 As shown in Figure S1, the conditions during the post-monsoon campaign were much more stagnant
227 than the pre-monsoon campaign. The VC was on average 4.5 times higher during the pre-monsoon
228 campaign compared to the post-monsoon campaign (Table S2) in line with previous studies (Gani et
229 al., 2019; Saha et al., 2019). The more stagnant conditions during the post-monsoon campaign likely
230 traps nocturnal emissions and their reaction products close to the surface, allowing for a significant
231 build-up of concentrations.

232 3.2 Gas phase observations

233 Time series of the observed mixing ratios (ppbv) of NO, NO₂ and O₃ are shown in Figure 1, for the
234 pre- and post-monsoon campaigns. The campaign averaged diurnal profiles are shown in Figure S3
235 and the mean, median and maximum mixing ratios are given in Table S2. It should be noted that only
236 one week of data was available for the pre-monsoon period. During the post-monsoon campaign,
237 extremely high mixing ratios of NO were observed with a campaign maximum mixing ratio of ~870
238 ppbv during the early morning of the 1st of November. During the early part of the pre-monsoon
239 campaign, a large enhancement in NO was observed with mixing ratios around 400 ppbv (Figure S4),
240 followed by significantly lower concentrations throughout the rest of the campaign. The campaign-
241 average NO diurnal profile shows very high NO mixing ratios at night (pre-: ~ 50 ppbv, post-: ~300
242 ppbv), with low afternoon mixing ratios < 2 ppbv due to ozone titration. These high NO
243 concentrations at night likely reduce any night-time chemistry through reactions with NO₃ radicals
244 and ozone. NO₂ during the pre-monsoon was observed to increase as the boundary layer reduced in
245 the late afternoon, with a mid-afternoon minimum. During the post-monsoon, a double peak in
246 concentrations was observed, in line with increasing ozone in the morning, and increasing NO in the
247 afternoon. Ozone showed a strong diurnal variation across both campaigns, with average afternoon
248 mixing ratios ~ 75 ppbv with pre- and post-monsoon maximums of 182 ppbv and 134 ppbv
249 respectively. Night-time O₃ concentrations were significantly higher during the pre-monsoon
250 campaign, likely due to the significantly lower NO concentrations.

251 3.3 Particle phase observations

252 The sampling site was heavily polluted in terms of particulate matter. The mean $\pm \sigma$ PM_{2.5}
253 concentration (Table S2) during the pre-monsoon campaign was (141 \pm 31) $\mu\text{g m}^{-3}$ with a spike in
254 concentrations of 672 $\mu\text{g m}^{-3}$ on the 01/6/2018 at 21:00 (Figure 1). The diurnal (Figure S5) shows
255 concentrations generally flat throughout the day. During the post-monsoon campaign, the average
256 PM_{2.5} concentration was higher at (182 \pm 94) $\mu\text{g m}^{-3}$, with a spike in concentrations of 695 $\mu\text{g m}^{-3}$ at
257 the end of the campaign (Figure 1). The diurnal shows a mid-afternoon minimum with high morning
258 and night concentrations. HR-AMS was used to measure the PM₁ sulfate and total organics.
259 Campaign averaged total organics concentrations were approximately double in the post-monsoon
260 (48.7 \pm 35.4) $\mu\text{g m}^{-3}$ compared to the pre-monsoon (19.8 \pm 13.7) $\mu\text{g m}^{-3}$. During the pre-monsoon
261 campaign, concentrations are generally flat throughout the day, with an increase in the late
262 afternoon, likely as the boundary layer decreases (Figure S5). During the post-monsoon, a much
263 more prominent diurnal is observed, with a mid-day minimum and high night-time concentrations.

264 This diurnal is likely driven by boundary layer conditions. Sulfate averaged (7.5 ± 1.8) $\mu\text{g m}^{-3}$ during
 265 the pre-monsoon campaign, with slightly lower average concentrations observed in the post-
 266 monsoon: (5.6 ± 2.7) $\mu\text{g m}^{-3}$ as shown in Figure S5. The sulfate diurnal variations are similar to those
 267 of the organic aerosol.

268

269

270

271

272

273

274

275

276

277

278

279

280

281

282

283

284

285

287

288

289

290

291

292

293

294

295

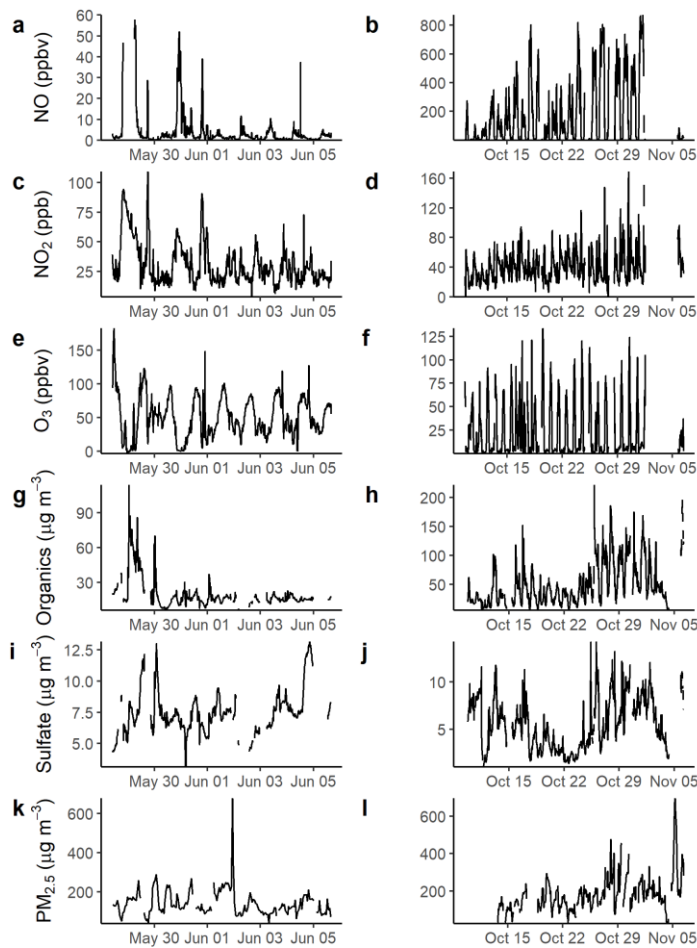


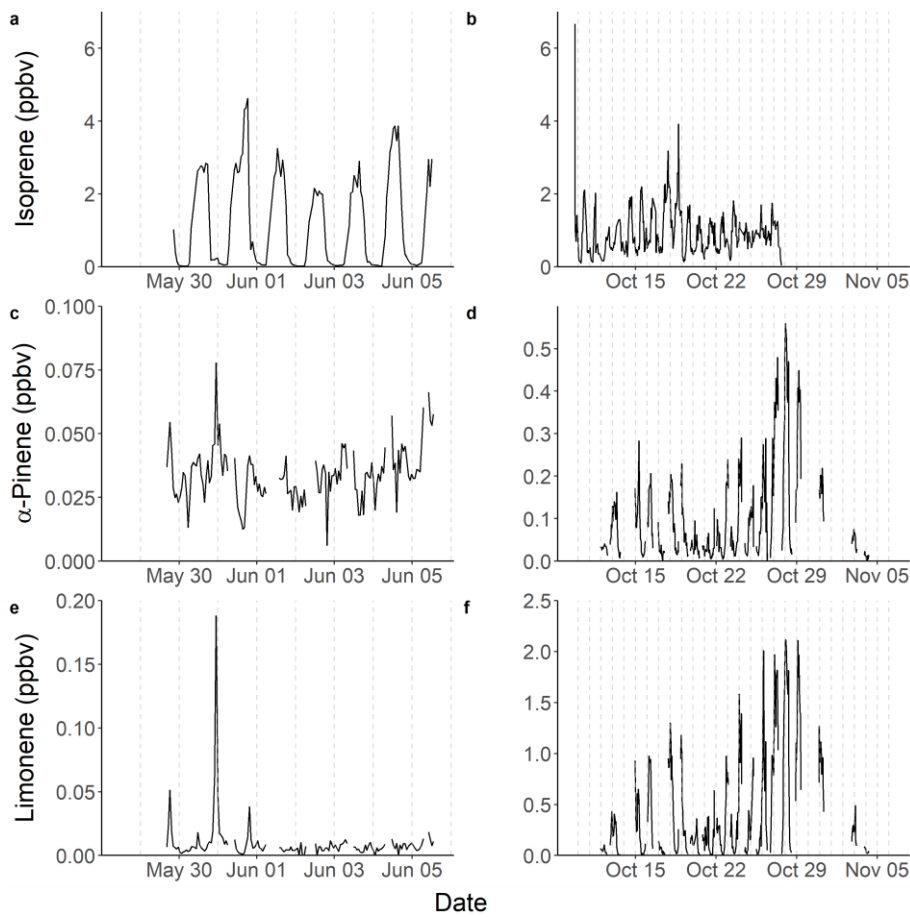
Figure 1. Time series of pollutants across the pre- (a,c,e,g,i) and post-monsoon (b,d,f,h,j) campaigns. During the pre-monsoon, NO concentrations were filters to below 60 ppbv, due to a large enhancement in concentrations at the start of the campaign, the full time series is shown in Figure S4. NO, NO₂, O₃ and HR-AMS – SO₄²⁻ were averaged to 15 minutes. PM_{2.5} was measured hourly.

296
297
298
299
300
301
302
303
304
305
306
307
308
309
310
311
312
313
314
315
316
317
318
319
320
321
322
323
324
325
326
327
328
329
330
331
332

3.4 Isoprene and monoterpene measurements

Isoprene was measured hourly using gas-chromatography with flame-ionisation-detection (GC-FID) across the two campaigns (Nelson et al., 2021), with the time series shown in Figure 2. The time series highlights similar diurnal variability each day, driven by biogenic emissions. Figure 3 shows the average diurnal profiles of isoprene during pre-monsoon (a) and post-monsoon (b). The mean isoprene mixing ratios were (1.22 ± 1.28) ppbv and (0.93 ± 0.65) ppbv, with maximum isoprene mixing ratios of 4.6 ppbv and 6.6 ppbv across the pre- and post-monsoon, respectively. This is in the same range as measured in Beijing (winter mean: (1.21 ± 1.03) ppbv, summer mean: (0.56 ± 0.55) ppbv, Acton et al., (2020)), Guangzhou (year round (1.14) ppbv) (Zou et al., 2019) and Taipei (summer daytime: (1.26) ppbv, autumn daytime: (0.38) ppbv) (Wang et al., 2013). The diurnal variability observed in the pre-monsoon period corresponds to a typical biogenic emission driven profile, with a rapid increase of isoprene around 05:00, reaching a peak around or after midday, before a nocturnal minimum. Figure 3 indicates that average daytime peak isoprene mixing ratios during the pre-monsoon campaign were roughly double that of the post-monsoon campaign. In contrast, average nocturnal mixing ratios of isoprene were 5 times higher in the post-monsoon compared to the pre-monsoon ((0.65 ± 0.43) ppbv versus (0.13 ± 0.18) ppbv). In the post-monsoon campaign, isoprene mixing ratios show a strong biogenic emission driven diurnal profile at the start of the campaign. However, towards the end of the post monsoon measurement period, the isoprene mixing ratios become less variable with a high mixing ratio maintained overnight (Figure 2). This is potentially due to more stagnant conditions as observed by the VC in Figure S1.

333
334
335
336

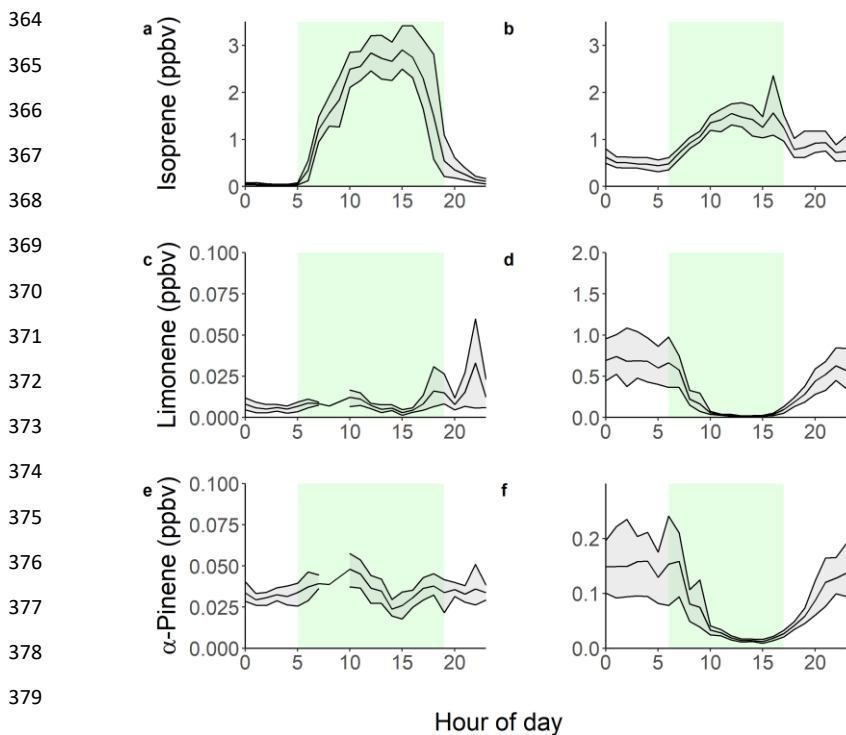


337
338
339
340

Figure 2. Time series across the pre- (left) and post-monsoon (right) campaigns of Isoprene (a,b), α -pinene (c,d), limonene (d,e). The vertical dotted lines represent midnight for each day.

341 A recent study in Delhi averaged across post-monsoon, summer and winter campaigns found that at
342 vegetative sites biogenic isoprene contributed on average 92 - 96 % to the total isoprene, while at
343 traffic dominated sites only 30 – 39 % of isoprene was from biogenic sources (Kashyap et al., 2019).
344 This is similar to the contributions of biogenic isoprene (40 %) to total isoprene mixing ratios at the

345 traffic dominated Marylebone Road London site.(Khan et al., 2018a) To gain some understanding of
 346 the sources of isoprene at our site in Delhi, the observed concentrations of isoprene were correlated
 347 to CO, which is an anthropogenic combustion tracer (Figure 54) similar to previous studies.(Khan et
 348 al., 2018a; Wagner and Kuttler, 2014) The isoprene concentrations were split between night and day
 349 (pre-monsoon; night: 19:00 – 05:00 h, day 05:00 – 19:00 h, post-monsoon; night: 17:00-06:00 h, day:
 350 06:00-17:00 h), based on the observed isoprene diurnals as shown in Figure 3. Isoprene correlated
 351 strongly with CO during the night across both campaigns (pre-monsoon: $R^2= 0.69$, post-monsoon:
 352 $R^2= 0.81$), but no correlation was observed during the day ($R^2 < 0.1$). This suggests that daytime
 353 isoprene is predominantly from biogenic sources, although a small amount will be from
 354 anthropogenic sources, and that nocturnal isoprene is emitted from anthropogenic sources, as seen
 355 in other locations. (Khan et al., 2018b; Panopoulou et al., 2020; Wang et al., 2013) The night-time
 356 isoprene mixing ratios (pre-monsoon: (0.13 ± 0.18) ppbv, post-monsoon: (0.65 ± 0.43) ppbv) were
 357 substantially higher than measured previously in Beijing and London (<50 pptv, (Bryant et al., 2020;
 358 Khan et al., 2018b)), but pre-monsoon concentrations were similar to those observed at night in
 359 Taipei (0.19 ppbv)(Wang et al., 2013). The high night-time concentrations during the post-monsoon
 360 period, towards the end of October are also likely influenced by the formation of a very low
 361 boundary layer, trapping pollutants near the surface, affecting all species similarly. An increase in
 362 biomass burning may also be a factor. Therefore, during the post-monsoon campaign a significant
 363 amount of isoprene oxidation products will be of anthropogenic origin.

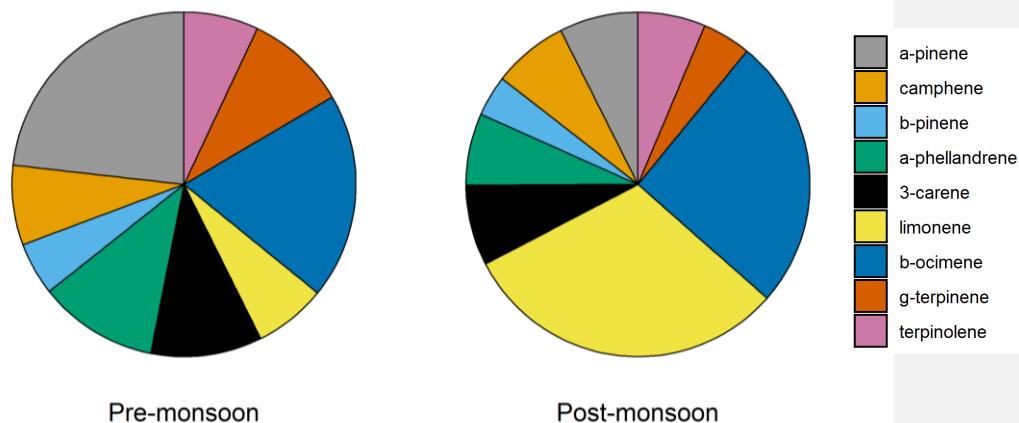


379
 380
 381
 Figure 3. Diurnal variations across the pre (left) and post-monsoon (right) campaigns of Isoprene (a,b), limonene (c,d) and α -pinene (e,f). The grey shaded area represents the 95 % confidence interval. The green shaded area represents the times driven by biogenic emissions, as defined by the isoprene diurnals.

382
383
384
385
386
387
388
389
390
391
392
393
394
395
396
397
398
399
400
401
402
403
404
405
406
407
408
409
410
411
412

Several monoterpenes were measured using GCxGC-MS. The time series of two monoterpenes, limonene and α -pinene, are shown in Figure 2. The α -pinene mixing ratio averaged (0.034 ± 0.011) ppbv during the pre-monsoon and (0.10 ± 0.11) ppbv during the post monsoon periods. This is in comparison to limonene, which averaged (0.01 ± 0.02) ppbv and (0.42 ± 0.51) ppbv across the pre- and post-monsoon campaigns, respectively. A strong diurnal variation was observed for both monoterpenes during the post-monsoon, peaking during the night (Figure 3), with a midday minimum. Nocturnal mixing ratios of the two monoterpenes were substantially higher during the post-monsoon (Limonene: (0.59 ± 0.11) ppbv, α -pinene: (0.13 ± 0.12) ppbv) than the pre-monsoon (Limonene: (0.011 ± 0.025) ppbv, α -pinene: (0.033 ± 0.009) ppbv) period. [The diurnal variations across both campaigns are likely driven by both emissions as well as boundary layer effects. The boundary layer effect however is much stronger during the post-monsoon, with a shallower nocturnal boundary layer, as such the post-monsoon period has a more pronounced diurnal. This diurnal again is likely driven by boundary layer dynamics. During the pre-monsoon, limited diurnal variability was observed compared to the post-monsoon.](#) Limonene was dominated by 3 short lived spikes in concentrations towards the start of the campaign (Figure 2). α -pinene concentrations generally increased during the morning, before decreasing during the afternoon. [A Multiple further 10 monoterpenes were measured concurrently using GCxGC-MS \(Nelson et al., 2021; Stewart et al., 2021c\). For all MT species, the post monsoon period had higher mean mixing ratios, with large nocturnal enhancements in mixing ratios. There are likely multiple factors leading the higher concentrations during the post-monsoon, including accumulation due to boundary layer effects, a lack of nocturnal radical chemistry and an increase in biomass burning \(Jain et al., 2014\). The average isomeric speciation of the measured monoterpenes showed low variability between day and night-time samples during each campaign, but significant differences were observed between the campaigns \(Figure 4\). Higher contributions from limonene and \$\beta\$ -ocimene were observed during the post-monsoon compared to the pre-monsoon. The reason for the difference in composition is likely due to differences in sources and/or sinks between the two periods.](#)

413



414

415

416 Figure 4. Average composition of monoterpenes across the pre-monsoon and post-monsoon
 417 periods.

418

419

420

421

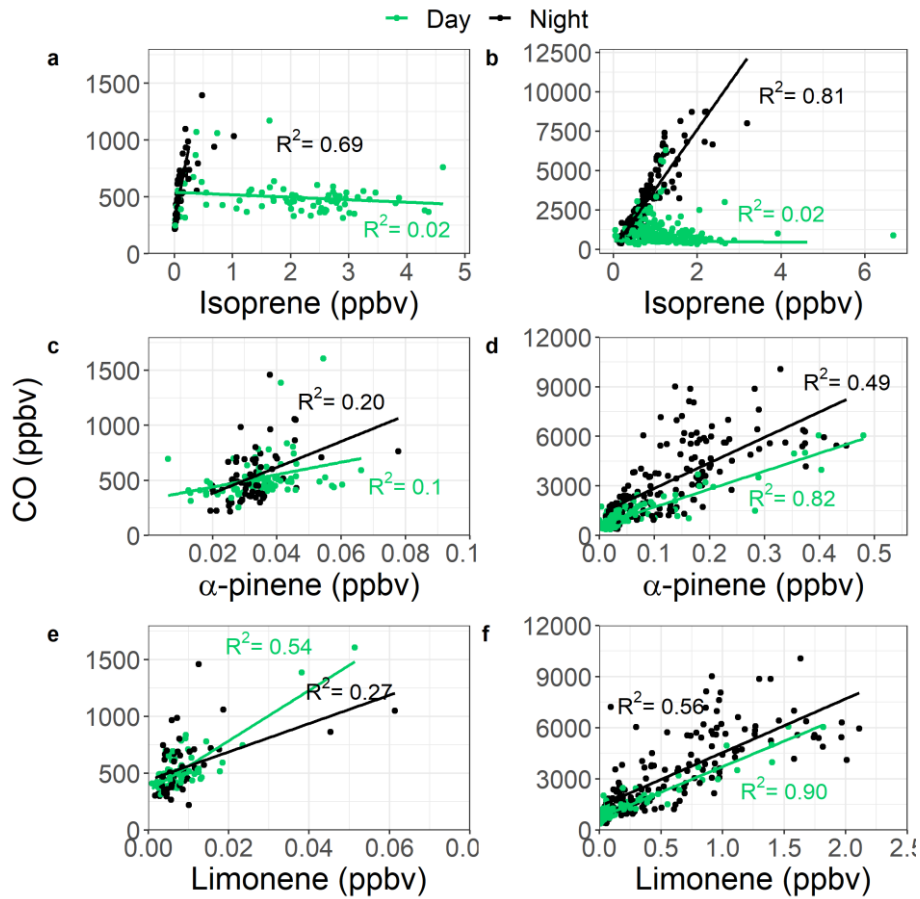
422

423

424

425

426 During the post-monsoon, α -pinene and limonene correlated strongly with CO during the day (α -
 427 pinene; $R^2 = 0.82$, limonene; $R^2 = 0.90$) and moderately at night (α -pinene; $R^2 = 0.49$, limonene; $R^2 =$
 428 0.56) as shown in Figure 54, suggesting anthropogenic sources. Other potentially important
 429 anthropogenic monoterpene sources include biomass burning, cooking and the use of personal
 430 care/volatile chemical products (Coggon et al., 2021; Gkatzelis et al., 2021; Hatch et al., 2019; Klein
 431 et al., 2016). The shallow nocturnal boundary layers across both campaigns leads to relatively high
 432 concentrations of total monoterpenes, with a maximum mixing ratio of 6 ppbv observed during the
 433 post-monsoon (Stewart et al., 2021c). After sunrise, the expanding boundary layer dilutes the high
 434 concentrations alongside increasing OH concentrations from photolytic sources such as the
 435 photolysis of HONO and carbonyls which likely causes a rapid decrease in the monoterpene mixing
 436 ratios. (Lelieveld et al., 2016)



438

439

Figure 54. Correlations between Isoprene, limonene and α -pinene with CO across the pre (left) and post-monsoon (right) campaigns. The samples are split between daytime (green) and nighttime (black) as defined by the Isoprene diurnals in Figure 3.

440

441

442

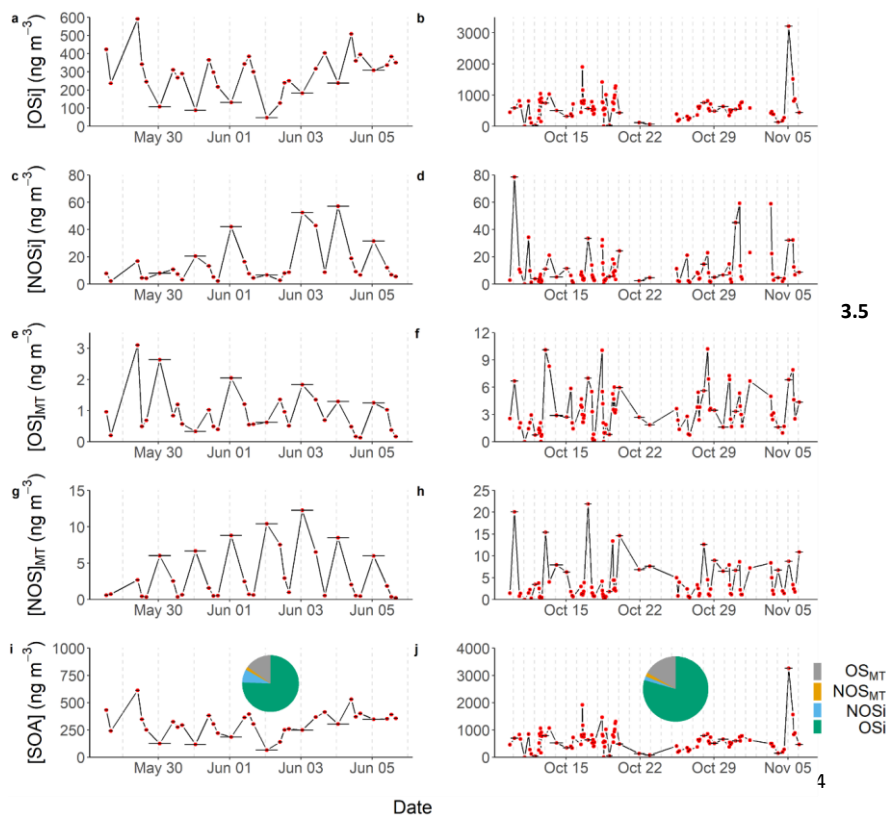
443

444

445

446

447
448
449



3.5

465
466
467
468
469
470
471

Figure 6.5. Time series across the pre- (left) and post-monsoon (right) campaigns of the quantified SOA tracers: OSI (a,b), NOSi (c,d), OS_{MT} (e,f), NOS_{MT} (g,h) and the sum of all SOA tracers (i,j) with the average campaign contributions. The vertical dotted lines represent midnight for each day. Only species identified in more than 40 % of the samples for each campaign were included.

Isoprene and monoterpene OS and NOS Secondary organic aerosol formation

472 At the measured concentrations, monoterpenes and isoprene are an important source of ozone and
473 OH reactivity at this site (Nelson et al., 2021). The resultant oxidised products will also be a key
474 source of SOA production. The UHPLC-MS² analysis identified and quantified 75 potential markers
475 across four classes of SOA, isoprene OS (OSi) and NOS (NOSi) derived species and monoterpene OS
476 (OS_{MT}) and NOS (NOS_{MT}) species. Figure 6.5 shows the contribution to the total quantified SOA

477 (qSOA), which consists of the time averaged sum of the four SOA classes (OSi, NOSi, OS_{MT}, NOS_{MT}),
478 across the pre- and post-monsoon campaigns. OSi species were the dominant SOA class quantified in
479 this study, contributing 75.6 % and 79.4 % of the qSOA across the pre- and post-monsoon campaigns
480 respectively. NOSi species contributed significantly more to the qSOA during the pre-monsoon (7.6
481 %) compared to the post-monsoon (2.1 %) period. Similar contributions from the monoterpene
482 derived SOA species were observed across both campaigns.

483 3.5.1 Isoprene SOAOS and NOS markers

484 OSi species are predominantly formed by photo-oxidation of isoprene by OH radicals with the
485 subsequent products formed dependent on ambient NO concentrations (Wennberg et al., 2018).
486 The pathways are split into high-NO and low-NO, although the NO concentrations that constitute
487 high and low are a sliding scale depending on the amount of reactivity (defined as $[\text{OH}] \times k_{\text{OH}}$)
488 (Newland et al., 2021). Under low-NO conditions, isoprene epoxydiol isomers (IEPOX) (Paulot et al.,
489 2009) are formed which can then undergo reactive uptake to the particle phase by acid-catalysed
490 multiphase chemistry involving inorganic sulfate, to form 2-MT-OS (Lin et al., 2012; Riva et al., 2019;
491 Surratt et al., 2010). Under high-NO conditions, 2-methyl glyceric acid is the dominant gas-phase
492 marker produced, which can undergo reactive uptake to the particle phase to form 2-MG-OS (Lin et
493 al., 2013a; Nguyen et al., 2015; Surratt et al., 2006, 2010).

494 A total of 21 potential OSi C₂₋₅ markers previously identified in chamber studies (Nguyen et al., 2010;
495 Riva et al., 2016a; Surratt et al., 2007, 2008b) and other ambient studies (Bryant et al., 2020;
496 Budisulistiorini et al., 2015; Hettiyadura et al., 2019; Kourtchev et al., 2016; Rattanavaraha et al.,
497 2016a; Wang et al., 2018b, 2021b) were quantified in the collected ambient samples. It should be
498 noted that several of the smaller (C₂₋₃) OSi tracers likely form from glyoxal, methylglyoxal and
499 hydroxyacetone as well as isoprene, and as such present a potential non-isoprene source of OSi
500 (Galloway et al., 2009; Liao et al., 2015).

501 Figure 65 shows the time series of total OSi concentrations observed across pre- (left, 5a) and post-
502 (right, 5b) monsoon campaigns. Total OSi time averaged concentrations (Table 1) were c.a. 2.3 times
503 higher during the post-monsoon ($\sim 556.6 \pm 422.5 \text{ ng m}^{-3}$) campaign than the pre-monsoon campaign
504 ($\sim 237.8 \pm 118.4 \text{ ng m}^{-3}$). These concentrations are similar to those observed in Beijing during summer
505 2017 (237.1 ng m^{-3} , (Bryant et al., 2020)), but higher than those observed in Shanghai in 2018 (40.4
506 ng m^{-3}) and 2019 (34.3 ng m^{-3}) (Wang et al., 2021b). As previously discussed, OSi species have been
507 shown to form via the gas-phase photo-oxidation of isoprene, with the reactive uptake of the
508 oxidised species into the particulate phase via sulfate (Lin et al., 2013a; Surratt et al., 2010).
509 Recently, a heterogeneous photo-oxidation pathway from 2-MT-OS (C₅H₁₂O₇S) to several OSi species
510 was proposed, including C₅H₁₀O₇S, C₅H₈O₇S, C₅H₁₂O₈S, C₅H₁₀O₈S and C₄H₈O₇S (Chen et al., 2020). 2-
511 MT-OS showed moderate correlations (pre-monsoon : R² = 0.52-0.72, post-monsoon: R² = 0.14-0.35)
512 with these OSi tracers that were lower than observed in Beijing summer (R² = 0.83-0.92) (Bryant et
513 al., 2020). These correlations could suggest that this is a more common formation route in pre-
514 monsoon Delhi, than in post-monsoon. However, the correlations could also be driven by the
515 common pathways between the OSi species, with the reactive uptake of gas phase intermediates via
516 sulfate reactions. The lower correlations during the post-monsoon could be due to increased
517 influences of anthropogenic sources coupled to the stagnant conditions.

518 Figure 76 shows the binned OSi concentrations for each filter collection time across the pre- and
519 post-monsoon campaigns to create a partial diurnal profile. During the pre-monsoon, the daily
520 variation in OSi concentrations was much clearer, with day-time maxima and nocturnal minima,
521 which are in line with daily peak isoprene (Figure 3) and OH radical concentrations. The highest

522 observed OSi concentrations during the pre-monsoon were $\sim 600 \text{ ng m}^{-3}$, which occurred at the start
523 of the campaign. High isoprene concentrations may have been the cause, but unfortunately isoprene
524 measurements were not available during this period to confirm. However, high OSi concentrations
525 also occurred when particulate inorganic sulfate concentrations were at their highest (Figure S6),
526 while sulfate measured via the HR-AMS was also high during this period (Figure 1). During the post-
527 monsoon, although a similar diurnal pattern was observed, the variation was less pronounced, with
528 higher OSi concentrations observed at the start and end of the campaign (Figure 65). [Due to the](#)
529 [secondary nature of sulfate, the sulfate concentrations are less likely to be influenced by the](#)
530 [boundary layer effects, compared to directly emitted VOCs.](#) The low OSi concentrations during the
531 middle of the campaign, coincide with lower isoprene and inorganic sulfate concentrations, but also
532 low VC values, suggesting more stagnant conditions.

533 The sum of OSi species across all filters sampled showed a variable correlation with particulate
534 sulfate across both campaigns. The pre-monsoon correlation was similar to those observed in
535 Beijing, Guangzhou and the SE-US ($R^2: 0.55$) (Bryant et al., 2020, 2021; Budisulistiorini et al., 2015;
536 Rattanavaraha et al., 2016a) while the post-monsoon was significantly weaker ($R^2: 0.28$). However, a
537 clear relationship between OSi tracers and inorganic sulfate can be seen in Figure 87 across both
538 campaigns, where the highest OSi concentrations occurred under the highest SO_4^{2-} particulate sulfate
539 concentrations. During the post-monsoon campaign, OSi concentrations levelled off at high sulfate
540 concentrations. In the pre-monsoon this levelling off is not observed, potentially due to the lower
541 number of samples. The high concentrations of organics measured by the HR-AMS (Table S2) during
542 the post-monsoon ($48.7 \pm 35.4 \mu\text{g m}^{-3}$) compared to the pre-monsoon ($19.8 \pm 13.7 \mu\text{g m}^{-3}$), suggests
543 the reactive uptake of the gaseous OSi intermediates to the aerosol phase may be limited due to
544 extensive organic coatings on the sulfate aerosol. Multiple studies have now shown that organic
545 coatings on sulfate aerosol can limit the reactive uptake of IEPOX, suggesting the pre-monsoon is
546 volume limited but the post-monsoon is diffusion limited. (Gaston et al., 2014; Lin et al., 2014; Riva
547 et al., 2016c)

548 Isoprene NOS (NOSi) have been shown to be produced by photo-oxidation in the presence of NO
549 and from NO_3 oxidation chemistry (Hamilton et al., 2021; Ng et al., 2017; Surratt et al., 2008b). Ten
550 different NOSi tracers were screened for across the two campaigns, with eight identified in the pre-
551 monsoon and ten in the post-monsoon. These tracers included: mono-nitrated ($\text{C}_5\text{H}_9\text{O}_{10}\text{NS}$,
552 $\text{C}_5\text{H}_{11}\text{O}_9\text{NS}$, $\text{C}_5\text{H}_{11}\text{O}_8\text{NS}$), di-nitrated ($\text{C}_5\text{H}_{10}\text{O}_{11}\text{N}_2\text{S}$), and tri-nitrated ($\text{C}_5\text{H}_9\text{O}_{13}\text{N}_3\text{S}$) species. These tracers
553 have been identified previously in China (Bryant et al., 2020, 2021; Hamilton et al., 2021; Wang et
554 al., 2018b, 2021b). Unlike the OSi tracers, total NOSi concentrations were on average higher during
555 the pre-monsoon ($32.6 \pm 19.9 \text{ ng m}^{-3}$) compared to the post-monsoon ($20.2 \pm 13.3 \text{ ng m}^{-3}$). This is
556 likely due to extremely high night-time NO concentrations during the post-monsoon quenching NO_3
557 radicals, limiting the isoprene + NO_3 pathway. The NOSi time series and diurnal shown in Figures 5
558 and 6 respectively highlight the strong nocturnal enhancements in concentrations during the pre-
559 monsoon, suggesting isoprene + NO_3 formation pathway is dominant. Due to the long sampling time,
560 it is likely that these species are forming in the early evening as NO_3 oxidation becomes more
561 competitive with OH, while isoprene concentrations are still relatively high. During the post-
562 monsoon, NOSi concentrations were highest at night and the early morning. The high morning
563 concentrations could be due to non-local sources mixing down as the shallow night-time boundary
564 layer breaks down. Ideally, future work in Delhi or India should focus on the measurements of
565 radicals and OH reactivity (k_{OH}), in order to improve our understanding of the chemistry occurring in
566 extremely polluted environments. A large spike in NOSi concentrations is observed at the start of the
567 post-monsoon campaign, which was not observed for the OSi tracers, this coincides with lower NO
568 concentrations than the rest of the post-monsoon campaign, reducing the NO_3 quenching by NO,

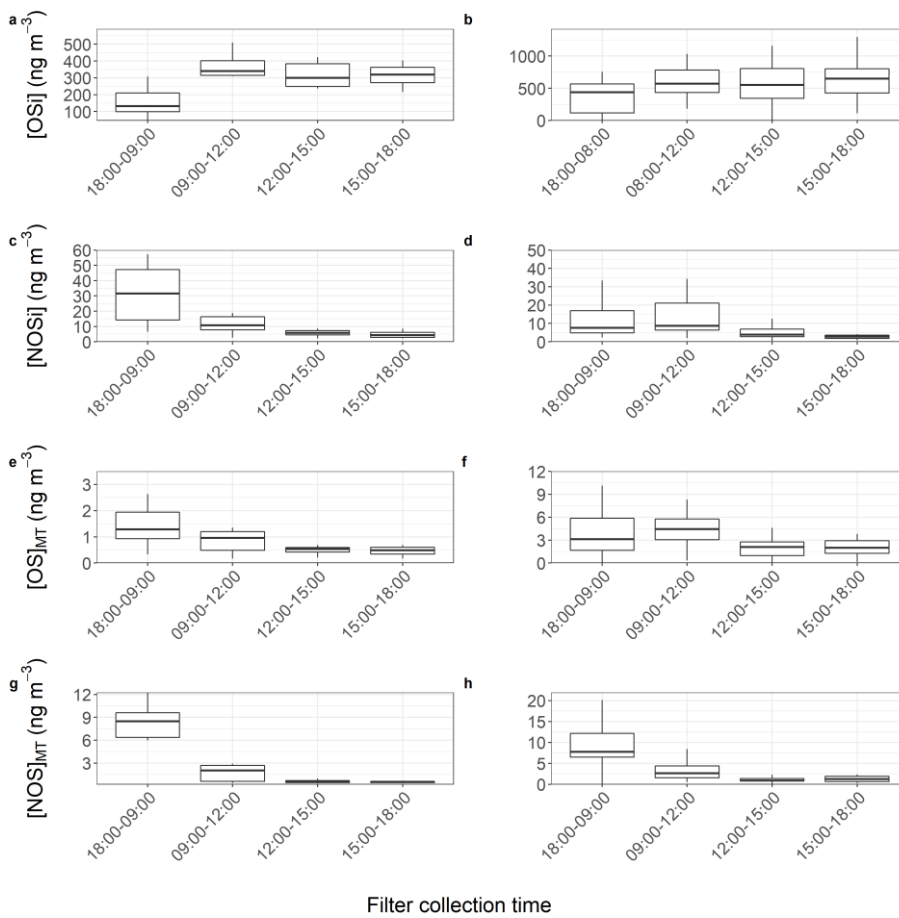
569 allowing for more isoprene + NO₃ oxidation. The NOSi species did not correlate towards particulate
 570 sulfate ($R^2 < 0.2$) across either campaign, suggesting that uptake onto sulfate is not the limiting step
 571 in NOSi formation (unlike for the OSi species).

572

573

574

575

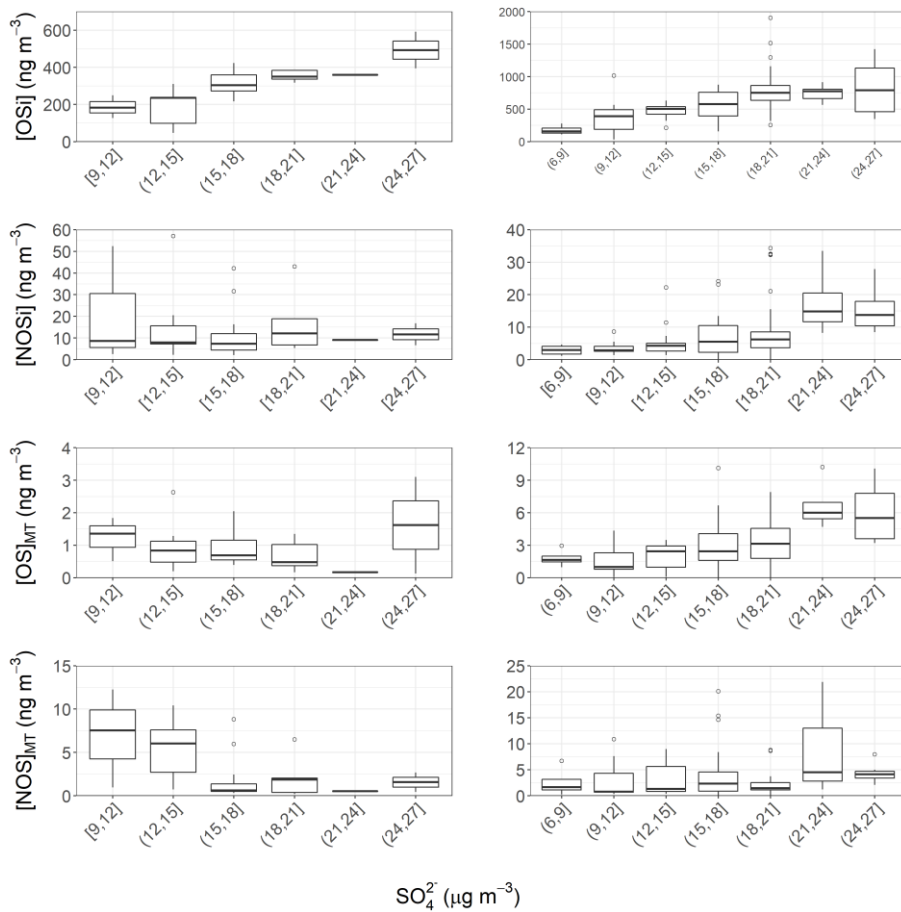


576

577

578

Figure 76. Partial diurnal variations from the binned concentrations of OSi, NOSi, OS_{MIT} and NOS_{MIT} concentrations at each filter collection time across the pre (left) and post-monsoon (right) campaigns. The lower and upper part of the box representing the 25th and 75th percentiles, with the upper and lower lines extending no further than 1.5 times the interquartile range of the highest and lowest values within the hinge respectively. Only species identified in more than 40 % of the samples for each campaign were included.



579

580

581

582

583

584

585

586

587

588

Figure 8-7. Quantified SOA (OS_i , NOS_i , OS_{MT} , NOS_{MT}) vs inorganic sulfate concentrations across the pre- (left) and post-monsoon (right) campaigns. The lower and upper part of the box representing the 25th and 75th percentiles, with the upper and lower lines extending no further than 1.5 times the interquartile range of the highest and lowest values within the hinge respectively. Only species identified in more than 40 % of the samples for each campaign were included.

590 3.5.28 Monoterpene secondary organic aerosol OS and NOS markers

591 Monoterpene derived OS (OS_{MT}) and NOS (NOS_{MT}) markers have also been identified from the
592 oxidation by OH, NO_3 and O_3 in the presence of SO_2 or sulfate seed in simulation studies
593 (Brüggemann et al., 2020b; Iinuma et al., 2007; Kleindienst et al., 2006; Surratt et al., 2008a; Zhao et
594 al., 2018). Compared to isoprene, the ozonolysis of monoterpenes is a key degradation pathway,
595 with higher SOA yields from ozonolysis observed when compared to isoprene (Åsa M. Jonsson et al.,
596 2005; Atkinson and Arey, 2003; Eddingsaas et al., 2012a, 2012b; Kristensen et al., 2013; Mutzel et
597 al., 2016; Simon et al., 2020; Zhao et al., 2015). A recent study in the SE-US suggests that the
598 degradation of 80 % of monoterpenes at night is due to ozonolysis at that location (Zhang et al.,
599 2018). Monoterpene derived OS and NOS species have been extensively observed, with ON
600 contributing considerably to OA (Lee et al., 2016; Xu et al., 2015; Zhang et al., 2018). Recently NOS
601 hydrolysis has also been shown to be a potential formation route of OS particle phase species (Darer
602 et al., 2011; Passananti et al., 2016).

603 Twenty-three monoterpene-derived organosulfate (OS_{MT}) species, which have been seen previously
604 in chamber (Surratt et al., 2008b) and ambient studies (Brüggemann et al., 2019; Wang et al., 2018b,
605 2021b), were identified across the pre- and post-monsoon campaigns. It should be noted that
606 recently OS_{MT} artefacts has been shown to form when filters have been sampled without a denuder.
607 (Brüggemann et al., 2020b). However, the strong diurnal variations of the OS_{MT} species, and lack of
608 correlation with SO_2 suggest this process is unlikely to have contributed significantly to the OS_{MT}
609 measured in this study. Post-monsoon concentrations were similar (3.96 ± 1.6) $ng\ m^{-3}$ to the pre-
610 monsoon (3.05 ± 1.3) $ng\ m^{-3}$, with $C_9H_{16}O_6S$ the dominant species across both campaigns,
611 contributing on average ~ 29 % of the OS_{MT} mass. [C₉H₁₆O₆S has been observed in chamber studies](#)
612 [\(Surratt et al., 2008a\) as well as in ambient samples in Denmark, Shanghai and Guangzhou](#)
613 [previously](#) (Bryant et al., 2021; Nguyen et al., 2014; Wang et al., 2017). It should be noted that the
614 majority of the OS_{MT} were not identified in every sample, and as such only tracers which were
615 identified in at least 40 % of the samples were examined further.

616 Total OS_{MT} showed a strong diurnal profile across both campaigns, peaking at night, with an
617 afternoon minimum (Figures 5 & 6). During the pre-monsoon campaign, the highest OS_{MT}
618 concentrations were observed during a day-time sample, coinciding with peak sulfate and NO
619 concentrations. Both limonene and α -pinene also show peaks during this filter sampling period of \sim
620 0.05 ppbv. Spikes in limonene and α -pinene concentrations were also observed on the 31st of May,
621 but OS_{MT} concentrations were much lower, likely due to the lower sulfate concentrations. During the
622 post-monsoon campaign, nocturnal enhancements are observed (Figure 7), suggesting MT + NO_3
623 chemistry is important. Like the $NOSi$ markers, higher OS_{MT} concentrations were observed during the
624 early morning sample, likely due to a lower PBLH concentrating the markers coupled to MT+OH/ O_3
625 occurring after sunrise in the post-monsoon. The night-time formation of the OS_{MT} species is in line
626 with previous studies (Bryant et al., 2021), and with the diurnal variations of α -pinene and limonene,
627 which peak at night. Previous chamber studies investigating reactions of monoterpenes with NO_3
628 radicals have also shown formation of OS_{MT} with the same molecular formulae as measured here
629 (Surratt et al., 2008a).

630 OS_{MT} concentrations observed in Delhi are much lower than those of the OSi , similar to other studies
631 (Hettiyadura et al., 2019; Wang et al., 2018b, 2021b). Considering the high concentrations of
632 extremely reactive α -pinene and limonene observed during the post-monsoon period, higher OS_{MT}
633 concentrations might be expected. One possible reason for the low OS_{MT} is the inability of OS_{MT}

634 precursor species to undergo reactive uptake into the aerosol phase under atmospherically relevant
635 acidic conditions, with chamber studies suggesting extremely acidic conditions are needed for
636 uptake to occur (Drozd et al., 2013). Delhi is characterised by large concentrations of free ammonia
637 and alkaline dust, and previous studies have highlighted that it has less acidic aerosol (pH 5.7 – 6.7,
638 Kumar et al., 2018) across the year than Beijing (pH 3.8 – 4.5, Ding et al., 2019) and the SE-US (pH 1.6
639 – 1.9, Rattanavara et al., 2016a).

640 Unlike the OS_{MT} species, the NOS_{MT} species (C₁₀H₁₇NO₇S, C₉H₁₅NO₈S, C₁₀H₁₇NO₉S, C₉H₁₅NO₉S,
641 C₁₀H₁₇NO₈S) showed strong seasonality, with pre- and post-monsoon concentrations of (7.6 ± 3.8) ng
642 m⁻³ and (17.6 ± 6.1) ng m⁻³ respectively. This is opposite to the quantified NOS_i species, which
643 showed higher pre-monsoon concentrations. This is likely due to much higher post-monsoon
644 concentrations of monoterpenes. Of the NOS_{MT} species observed, C₁₀H₁₇NO₇S was the most
645 abundant, contributing on average 79 % and 76 % of the NOS_{MT} concentrations across the pre- and
646 post-monsoon respectively. Previous studies have also highlighted C₁₀H₁₇NO₇S to be the dominant
647 monoterpene derived sulfate containing tracer (Wang et al., 2018b). In the post-monsoon nine
648 C₁₀H₁₇NO₇S isomers were observed, and seven in the pre-monsoon. The summed C₁₀H₁₇NO₇S
649 concentrations during the pre- (5.96 ± 3.33) ng m⁻³ and post-monsoon (13.36 ± 4.98) ng m⁻³, are of a
650 similar magnitude to those observed in other locations as shown in Table 2. These concentrations
651 are also similar to those quantified by authentic standards across four Chinese megacities (Wang et
652 al., 2021a). Like the OS_{MT} species, some NOS_{MT} species were not identified in many of the filter
653 samples, and as such tracers which were observed in more than 40 % of the samples were summed
654 for further analysis. The NOS_{MT} pre-monsoon time series (Figure 65) shows a similar temporal profile
655 to the NOS_i species, with lower concentrations during the enhancement in NO concentrations
656 (Figure S4) at the start of the campaign. NOS_{MT} showed strong diurnal variations across both
657 campaigns (Figure 76), peaking at night with lower concentrations during the afternoon, as seen
658 previously (Bryant et al., 2021; Wang et al., 2018b). Therefore, the formation of NOS_{MT} is likely
659 dominated by NO₃ radical chemistry. Both NOS_{MT} and OS_{MT} species showed limited correlation
660 towards SO₂ and particulate sulfate (R² < 0.1), indicating that although sulfate is essential to their
661 formation, sulfate availability does not control NOS_{MT} concentrations.

662

663 **3.5.340 Contributions of total-quantified total Isoprene and monoterpene OS and NOSSOA (qSOA)** 664 **to particulate mass**

665 Particulate concentrations in Delhi are among the highest across the world (WHO, 2018), with
666 concentrations over 600 µg m⁻³ being observed during this study. qSOA, defined here as the sum of
667 all OS_i, NOS_i, OS_{MT}, and NOS_{MT} tracers quantified (including those not identified in more than 40 % of
668 the samples), was calculated to determine the total contribution these species make to particulate
669 mass in Delhi. Total oxidised organic aerosol (OOA), a proxy for SOA in PM₁, was derived from the
670 HR-AMS measurements during the pre- and post-monsoon campaigns, with averages of (19.8 ± 13.7)
671 µg m⁻³ and (48.7 ± 35.4) µg m⁻³ respectively. qSOA contributed on average (2.0 ± 0.9) % and (1.8 ±
672 1.4) % to the total OOA. Isoprene and monoterpene derived species contributed on average 83.2 %
673 and 16.8 % of qSOA across the pre-monsoon respectively compared to 81.5 % and 18.5 % during the
674 post-monsoon respectively. During certain periods qSOA contributed a maximum of 4.2 % and 6.6 %
675 to OOA during the pre- and post-monsoon, respectively. This is under the assumption that when the
676 OS and NOS species fragment in the AMS ion source they lose their sulfate and nitrate groups. This is
677 similar to the contributions made by OS_i markers in Beijing to total OOA (2.2 %) (Bryant et al., 2020).
678 Previous studies in the SE-US have reported much higher contributions of isoprene species to total
679 OA. As quantified by an aerosol chemical speciation monitor, summed iSOA tracers on average

680 accounted for 9.4 % of measured OA at Look Rock, downwind of Maryville and Knoxville, but up to a
681 maximum of 28.1 % (Budisulistiorini et al., 2015). This is lower than that measured at a rural site at
682 Yorkville, Georgia with just low-NO isoprene SOA tracers accounting for between 12-19 % of total OA
683 (Lin et al., 2013b).

684 Sulfate was also measured in the PM₁ size range by HR-AMS, with pre- and post-monsoon mean
685 concentrations of $(7.5 \pm 1.8) \mu\text{g m}^{-3}$ and $(5.5 \pm 2.7) \mu\text{g m}^{-3}$. The sulfate containing OS and NOS species
686 quantified in this study may fragment in the AMS to produce a sulfate signal which is not related to
687 inorganic sulfate. To estimate the contribution that sulfate contained within qSOA species could
688 make to total AMS sulfate, the quantified mass of sulfate contained within each marker was
689 calculated based on the fraction of sulfate to each marker molecular mass. For example, 2-MT-OS
690 has an accurate mass of m/z 216.21, meaning the percentage of 2-MT-OS mass associated with
691 sulfate is ~44 %. During the pre-monsoon campaign the qSOA sulfate accounted for on average 2.2
692 % to the total PM₁ sulfate, but up to 4.8 % on certain days. qSOA contributed considerably more to
693 the sulfate in the post-monsoon campaign, with an average of $(6.1 \pm 4.5) \%$ with a maximum of 18.7
694 %. This finding indicates the need to consider the sources of particulate sulfate measured by the
695 AMS when calculating aerosol pH. The sulfate contribution from the fragmentation of common small
696 OS compounds (hydroxymethylsulfonate, methylsulfonic acid) can be distinguished in the AMS using
697 the relative ratio of sulfur containing peaks.(Chen et al., 2019; Javed et al., 2021) However, more
698 work is needed to determine how larger OS and NOS fragment in the AMS such as those quantified
699 in this study. Overall, this highlights that isoprene and MT oxidation can make significant
700 contributions to organic and sulfate-containing aerosol, even in extremely polluted environments
701 such as Delhi. It should be noted that this is just a subset of potentially many more SOA from
702 isoprene and monoterpene markers and only focusses on sulfate containing species.

703

704 **Conclusion**

705 Isoprene- and monoterpene-derived organosulfate (OS) and nitrooxy organosulfate (NOS) species
706 were quantified during pre- and post-monsoon measurement periods in the Indian megacity of
707 Delhi. An extensive dataset of supplementary measurements was obtained alongside filter samples,
708 including isoprene and speciated monoterpenes. Isoprene and monoterpene emissions were found
709 to be highly influenced by anthropogenic sources, with strong correlations to anthropogenic tracers
710 at night across both campaigns. High nocturnal concentrations of pollutants were observed due to a
711 low boundary layer height and stagnant conditions, especially during the post-monsoon period.

712 Isoprene OS markers (OS_i) were observed in higher concentrations during the post-monsoon ($557 \pm$
713 $423) \text{ ng m}^{-3}$ compared to the pre-monsoon campaign ($238 \pm 118) \text{ ng m}^{-3}$. OS_i showed a moderate
714 correlation with inorganic sulfate across both campaigns. However, concentrations levelled off at
715 high sulfate concentrations during the post-monsoon which is consistent with organic coatings
716 limiting uptake of isoprene epoxides. Isoprene NOS species (NOS_i) showed nocturnal enhancements
717 across both campaigns, while the highest average concentrations were observed in the morning
718 samples of the post-monsoon campaign. The high morning concentrations are likely due to the
719 oxidation of VOCs by OH radicals from photolytic processes throughout the morning. Monoterpene
720 derived OS (OS_{MT}) and NOS (NOS_{MT}) markers were observed to have nocturnal enhancements in
721 concentrations, in-line with their precursors. NOS_{MT} markers were observed in similar concentrations
722 to those of other megacities. Total quantified SOA contributed on average $(2.0 \pm 0.9) \%$ and $(1.8 \pm$
723 $1.4) \%$ to the total OOA. Considering high OOA concentrations were observed across the two
724 campaigns, the total markers contributed up to a maximum of 4.2 % and 6.6 % across the pre- and

725 post-monsoon respectively. Overall, this work highlights that even small numbers of isoprene and
 726 monoterpene derived SOA markers can make significant contributions to OA mass, even in highly
 727 polluted megacities.

728

729 Table 1. Molecular formulae, retention times and time weighted means (ng m^{-3}) of
 730 organosulfates (OS) and nitrooxy organosulfates (NOS) from isoprene (i) and monoterpenes
 731 (MT) observed across pre- and post-monsoon campaigns in Delhi.

Class	Molecular formula	Pre-	SD	Post-	SD	RT's (min)
OS _i	C ₅ H ₁₂ O ₇ S	38.79	30.19	17.91	19.87	0.71
	C ₅ H ₁₀ O ₅ S	26.16	23.30	53.63	131.19	0.93
	C ₂ H ₄ O ₆ S	21.35	18.27	84.65	82.79	0.73
	C ₅ H ₁₀ O ₆ S	19.80	13.78	45.87	29.47	0.79
	C ₄ H ₈ O ₇ S	19.70	12.48	47.96	39.01	0.73
	C ₃ H ₆ O ₅ S	19.50	12.47	35.27	40.15	0.73
	C ₅ H ₈ O ₇ S	18.76	11.01	38.75	25.34	0.73
	C ₄ H ₈ O ₆ S	16.57	9.77	45.48	37.46	0.74
	C ₅ H ₁₀ O ₇ S	11.82	7.04	25.89	18.06	0.73
	C ₃ H ₆ O ₆ S	6.64	5.00	38.06	40.30	0.73
	C ₄ H ₈ O ₅ S	6.46	4.08	22.44	21.39	0.75
	C ₅ H ₁₀ O ₈ S	6.25	5.07	7.00	5.54	0.73
	C ₂ H ₄ O ₅ S	5.33	3.37	15.92	13.79	0.73
	C ₂ H ₆ O ₅ S	5.23	6.36	24.99	20.38	0.73
	C ₅ H ₈ O ₅ S	5.16	2.57	7.87	7.93	0.85
	C ₃ H ₆ O ₇ S	3.54	3.49	14.78	11.50	0.75
	C ₅ H ₁₂ O ₆ S	2.01	1.23	6.53	4.32	0.74
	C ₃ H ₈ O ₆ S	1.90	1.08	12.25	10.82	0.75
	C ₅ H ₈ O ₉ S	1.20	1.04	2.12	1.85	0.64
	C ₄ H ₆ O ₆ S	1.10	0.76	8.61	15.65	0.74
C ₅ H ₁₂ O ₈ S	0.55	0.43	0.65	0.61	0.75	
Total		237.83		556.64		
NOS _i	C ₅ H ₁₀ O ₁₁ N ₂ S	18.65	8.77	11.63	8.09	1.39,1.92,2.85,3.4
	C ₅ H ₁₁ O ₉ NS	8.55	5.71	5.93	5.06	0.86
	C ₅ H ₉ O ₁₀ NS	3.91	3.46	1.42	1.31	0.94
	C ₅ H ₁₁ O ₈ NS	1.52	0.84	1.17	1.20	1.09
	C ₅ H ₉ O ₁₃ N ₃ S	0.002	0.001	0.011	0.009	6.67,7.89,8.06
Total		32.63		20.15		
OS _{MT}	C ₉ H ₁₆ O ₆ S	1.10	0.61	1.67	0.88	6.67/7.14/7.5/8.3
	C ₁₀ H ₁₈ O ₅ S	0.56	0.63	0.10	0.12	3.39
	C ₁₀ H ₁₆ O ₅ S	0.28	0.13	0.77	0.06	4.91/7/9.08/10.9/11.33/11.97/13.26
	C ₁₀ H ₂₀ O ₇ S	0.25	0.21	0.27	0.21	4.19
	C ₁₀ H ₁₆ O ₇ S	0.23	0.15	0.21	0.13	3.61/11.68
	C ₉ H ₁₆ O ₇ S	0.16	0.17	0.22	0.19	4.39/6.77

	C ₁₀ H ₁₈ O ₆ S	0.15	0.10	NA	NA	10.27
	C ₉ H ₁₄ O ₆ S	0.15	1.10	0.25	0.14	3.5/5.81
	C ₁₀ H ₁₆ O ₆ S	0.10	0.06	0.06	0.03	9.33
	C ₁₀ H ₁₈ O ₈ S	0.02	0.01	0.04	0.24	7.24
	C ₈ H ₁₄ O ₇ S	0.04	0.03	0.10	0.15	4.46
	Total	3.05		3.68		
NO _{S,WT}						9.1/10.16/10.67/10.92/11.07/11.36/11.57/12.01
	C ₁₀ H ₁₇ NO ₇ S	5.96	3.33	13.36	4.98	/13.28
	C ₉ H ₁₅ NO ₈ S	1.12	0.51	2.79	1.14	3.5/5.81
	C ₁₀ H ₁₇ NO ₉ S	0.47	0.19	1.15	0.29	3.93/5.34/6.39/7.89/9.26/10.11/17.94
	C ₉ H ₁₅ NO ₉ S	0.0216	0.0044	0.22	0.14	2.69/3.46
	C ₁₀ H ₁₇ NO ₈ S	0.01	0.01	0.07	0.04	5.77
	Total	7.59		17.59		

732

733

734

735

736

737

Table 2. Comparison of C₁₀H₁₇NO₇S concentrations across different locations. Locations and concentrations in bold were quantified by authentic standards.

738

Location	C ₁₀ H ₁₇ NO ₇ S (ng m ⁻³)	Reference
Delhi Pre-monsoon	5.96	This study
Delhi Post-monsoon	13.36	This study
Guangzhou summer	7.15	Bryant et al., 2021
Guangzhou winter	11.11	Bryant et al., 2021
Shanghai 15/16	6.21	Wang et al., 2021b
Shanghai 16/17	5.55	Wang et al., 2021b
Beijing	12.00	Wang et al., 2018b
Atlanta	9.00	Hettiyadura et al., 2019
Hong Kong	5.61	Wang et al., 2021a
Guangzhou	12.32	Wang et al., 2021a
Shanghai	16.51	Wang et al., 2021a
Beijing	13.15	Wang et al., 2021a

739

740 Data availability

741 Data used in this study can be accessed from the CEDA
 742 archive: <https://catalogue.ceda.ac.uk/uuid/ba27c1c6a03b450e9269f668566658ec> (Nemitz et al.,
 743 2020).

744 Author contributions

745 DJB prepared the manuscript with contributions from all authors. DJB, BSN, SJS, SHB, WSD, ARV,
746 JMC, WJFA, BL, EN and JRH provided measurements and data processing of pollutants used in this
747 study. MJN and ARR contributed to scientific discussion. S, RG, BRG, TH and EN assisted with
748 logistics. CNH, JDL, ARR, JFH provided overall guidance to the experimental setup and design.

749 **Acknowledgements**

750 The authors acknowledge Tuhin Mandal at CSIR-National Physical Laboratory for his support in
751 facilitating the measurement sites used in this project and Gareth Stewart for the VOC
752 measurements. This work was supported by the Newton Bhabha fund administered by the UK
753 Natural Environment Research Council through the DelhiFlux and ASAP projects of the Atmospheric
754 Pollution and Human Health in an Indian Megacity (APHH-India) programme. The authors gratefully
755 acknowledge the financial support provided by the UK Natural Environment Research Council and
756 the Earth System Science Organization, Ministry of Earth Sciences, Government of India, under the
757 Indo-UK Joint Collaboration (DelhiFlux). Daniel J. Bryant and Beth S. Nelson acknowledge the NERC
758 SPHERES doctoral training programme for studentships. James M. Cash is supported by a NERC E3
759 DTP studentship.

760 **Financial support**

761 This research has been supported by the Natural Environment Research Council (grant nos.
762 NE/P016502/1 and NE/P01643X/1) and the Govt. of India, Ministry of Earth Sciences (grant no.
763 MoES/16/19/2017/APHH, DelhiFlux).

764 **Competing interests**

765 The authors declare that they have no conflict of interest.

766 **References**

- 767 Anand, V., Korhale, N., Rathod, A. and Beig, G.: On processes controlling fine particulate matters in
768 four Indian megacities, *Environ. Pollut.*, 254, doi:10.1016/j.envpol.2019.113026, 2019.
- 769 Anon: Import Surface Meteorological Data from NOAA Integrated Surface Database (ISD) •
770 worldmet, [online] Available from: <https://davidcarslaw.github.io/worldmet/index.html> (Accessed
771 24 October 2021), n.d.
- 772 Åsa M. Jonsson, *, Mattias Hallquist, and and Ljungström, E.: Impact of Humidity on the Ozone
773 Initiated Oxidation of Limonene, Δ^3 -Carene, and α -Pinene, *Environ. Sci. Technol.*, 40(1), 188–194,
774 doi:10.1021/ES051163W, 2005.
- 775 Atkinson, R. and Arey, J.: Gas-phase tropospheric chemistry of biogenic volatile organic compounds:
776 A review, *Atmos. Environ.*, 37(SUPPL. 2), 197–219, doi:10.1016/S1352-2310(03)00391-1, 2003.
- 777 Balakrishnan, K., Dey, S., Gupta, T., Dhaliwal, R. S., Brauer, M., Cohen, A. J., Stanaway, J. D., Beig, G.,
778 Joshi, T. K., Aggarwal, A. N., Sabde, Y., Sadhu, H., Frostad, J., Causey, K., Godwin, W., Shukla, D. K.,
779 Kumar, G. A., Varghese, C. M., Muraleedharan, P., Agrawal, A., Anjana, R. M., Bhansali, A., Bhardwaj,
780 D., Burkart, K., Cercy, K., Chakma, J. K., Chowdhury, S., Christopher, D. J., Dutta, E., Furtado, M.,
781 Ghosh, S., Ghoshal, A. G., Glenn, S. D., Guleria, R., Gupta, R., Jeemon, P., Kant, R., Kant, S., Kaur, T.,
782 Koul, P. A., Krish, V., Krishna, B., Larson, S. L., Madhipatla, K., Mahesh, P. A., Mohan, V.,
783 Mukhopadhyay, S., Mutreja, P., Naik, N., Nair, S., Nguyen, G., Odell, C. M., Pandian, J. D.,
784 Prabhakaran, D., Prabhakaran, P., Roy, A., Salvi, S., Sambandam, S., Saraf, D., Sharma, M.,
785 Shrivastava, A., Singh, V., Tandon, N., Thomas, N. J., Torre, A., Xavier, D., Yadav, G., Singh, S.,
786 Shekhar, C., Vos, T., Dandona, R., Reddy, K. S., Lim, S. S., Murray, C. J. L., Venkatesh, S. and Dandona,
787 L.: The impact of air pollution on deaths, disease burden, and life expectancy across the states of

788 India: the Global Burden of Disease Study 2017, *Lancet Planet. Heal.*, 3(1), e26–e39,
789 doi:10.1016/S2542-5196(18)30261-4, 2019.

790 Bhandari, S., Gani, S., Patel, K., Wang, D. S., Soni, P., Arub, Z., Habib, G., Apte, J. S. and Hildebrandt
791 Ruiz, L.: Sources and atmospheric dynamics of organic aerosol in New Delhi, India: Insights from
792 receptor modeling, *Atmos. Chem. Phys.*, 20(2), 735–752, doi:10.5194/acp-20-735-2020, 2020.

793 Borbon, A., Fontaine, H., Veillerot, M., Locoge, N., Galloo, J. C. and Guillermo, R.: An investigation
794 into the traffic-related fraction of isoprene at an urban location, *Atmos. Environ.*, 35(22), 3749–3760,
795 doi:10.1016/S1352-2310(01)00170-4, 2001.

796 Brüggemann, M., van Pinxteren, D., Wang, Y., Yu, J. Z. and Herrmann, H.: Quantification of known
797 and unknown terpenoid organosulfates in PM10 using untargeted LC–HRMS/MS: contrasting
798 summertime rural Germany and the North China Plain, *Environ. Chem.*, 16(5), 333,
799 doi:10.1071/EN19089, 2019.

800 Brüggemann, M., Xu, R., Tilgner, A., Kwong, K. C., Mutzel, A., Poon, H. Y., Otto, T., Schaefer, T.,
801 Poulain, L., Chan, M. N. and Herrmann, H.: Organosulfates in Ambient Aerosol: State of Knowledge
802 and Future Research Directions on Formation, Abundance, Fate, and Importance, *Environ. Sci.*
803 *Technol.*, 54(7), 3767–3782, doi:10.1021/acs.est.9b06751, 2020a.

804 Brüggemann, M., Riva, M., Perrier, S., Poulain, L., George, C. and Herrmann, H.: Overestimation of
805 Monoterpene Organosulfate Abundance in Aerosol Particles by Sampling in the Presence of SO₂,
806 *Environ. Sci. Technol. Lett.*, 8, 206–211, doi:10.1021/acs.estlett.0c00814, 2020b.

807 Bryant, D. J., Dixon, W. J., Hopkins, J. R., Dunmore, R. E., Pereira, K. L., Shaw, M., Squires, F. A.,
808 Bannan, T. J., Mehra, A., Worrall, S. D., Bacak, A., Coe, H., Percival, C. J., Whalley, L. K., Heard, D. E.,
809 Slater, E. J., Ouyang, B., Cui, T., Surratt, J. D., Liu, D., Shi, Z., Harrison, R., Sun, Y., Xu, W., Lewis, A. C.,
810 Lee, J. D., Rickard, A. R. and Hamilton, J. F.: Strong anthropogenic control of secondary organic
811 aerosol formation from isoprene in Beijing, *Atmos. Chem. Phys.*, 20(12), 7531–7552,
812 doi:10.5194/acp-20-7531-2020, 2020.

813 Bryant, D. J., Elzein, A., Newland, M., White, E., Swift, S., Watkins, A., Deng, W., Song, W., Wang, S.,
814 Zhang, Y., Wang, X., Rickard, A. R. and Hamilton, J. F.: Importance of Oxidants and Temperature in
815 the Formation of Biogenic Organosulfates and Nitrooxy Organosulfates, *ACS Earth Sp. Chem.*,
816 *acsearthspacechem.1c00204*, doi:10.1021/ACSEARTHSPACECHEM.1C00204, 2021.

817 Budisulistiorini, S. H., Li, X., Bairai, S. T., Renfro, J., Liu, Y., Liu, Y. J., McKinney, K. A., Martin, S. T.,
818 McNeill, V. F., Pye, H. O. T., Nenes, A., Neff, M. E., Stone, E. A., Mueller, S., Knote, C., Shaw, S. L.,
819 Zhang, Z., Gold, A. and Surratt, J. D.: Examining the effects of anthropogenic emissions on isoprene-
820 derived secondary organic aerosol formation during the 2013 Southern Oxidant and Aerosol Study
821 (SOAS) at the Look Rock, Tennessee ground site, *Atmos. Chem. Phys.*, 15(15), 8871–8888,
822 doi:10.5194/acp-15-8871-2015, 2015.

823 Cash, J. M., Langford, B., Di Marco, C., Mullinger, N. J., Allan, J., Reyes-Villegas, E., Joshi, R., Heal, M.
824 R., Acton, W. J. F., Hewitt, C. N., Misztal, P. K., Drysdale, W., Mandal, T. K., Gadi, R., Gurjar, B. R. and
825 Nemitz, E.: Seasonal analysis of submicron aerosol in Old Delhi using high-resolution aerosol mass
826 spectrometry: chemical characterisation, source apportionment and new marker identification,
827 *Atmos. Chem. Phys.*, 21(13), 10133–10158, doi:10.5194/ACP-21-10133-2021, 2021a.

828 Cash, J. M., Langford, B., Di Marco, C., Mullinger, N. J., Allan, J., Reyes-Villegas, E., Joshi, R., Heal, M.
829 R., Acton, W. J. F., Hewitt, C. N., Misztal, P. K., Drysdale, W., Mandal, T. K., Shivani, Gadi, R., Gurjar, B.
830 R. and Nemitz, E.: Seasonal analysis of submicron aerosol in Old Delhi using high-resolution aerosol
831 mass spectrometry: Chemical characterisation, source apportionment and new marker
832 identification, *Atmos. Chem. Phys.*, 21(13), 10133–10158, doi:10.5194/ACP-21-10133-2021, 2021b.

833 Chan, M. N., Surratt, J. D., Chan, A. W. H., Schilling, K., Offenberg, J. H., Lewandowski, M., Edney, E.
834 O., Kleindienst, T. E., Jaoui, M., Edgerton, E. S., Tanner, R. L., Shaw, S. L., Zheng, M., Knipping, E. M.
835 and Seinfeld, J. H.: Influence of aerosol acidity on the chemical composition of Secondary Organic
836 Aerosol from β -caryophyllene, *Atmos. Chem. Phys. Discuss.*, 10(11), 29249–29289,
837 doi:10.5194/acpd-10-29249-2010, 2010.

838 Chen, Y., Xu, L., Humphry, T., Hettiyadura, A. P. S., Ovadnevaite, J., Huang, S., Poulain, L., Schroder, J.
839 C., Campuzano-Jost, P., Jimenez, J. L., Herrmann, H., O'Dowd, C., Stone, E. A. and Ng, N. L.: Response
840 of the Aerodyne Aerosol Mass Spectrometer to Inorganic Sulfates and Organosulfur Compounds:
841 Applications in Field and Laboratory Measurements, *Environ. Sci. Technol.*, 53(9), 5176–5186,
842 doi:10.1021/ACS.EST.9B00884/ASSET/IMAGES/MEDIUM/ES-2019-00884R_0003.GIF, 2019.

843 Chen, Y., Zhang, Y., T. Lambe, A., Xu, R., Lei, Z., E. Olson, N., Zhang, Z., Szalkowski, T., Cui, T., Vizuite,
844 W., Gold, A., J. Turpin, B., P Ault, A., Nin Chan, M. and D. Surratt, J.: Heterogeneous Hydroxyl Radical
845 Oxidation of Isoprene Epoxydiol-Derived Methyltetrol Sulfates: Plausible Formation Mechanisms of
846 Previously Unexplained Organosulfates in Ambient Fine Aerosols, *Environ. Sci. & Technol. Lett.*,
847 0(ja), doi:10.1021/acs.estlett.0c00276, 2020.

848 Cheng, X., Li, H., Zhang, Y., Li, Y., Zhang, W., Wang, X., Bi, F., Zhang, H., Gao, J., Chai, F., Lun, X., Chen,
849 Y. and Lv, J.: Atmospheric isoprene and monoterpenes in a typical urban area of Beijing: Pollution
850 characterization, chemical reactivity and source identification, *J. Environ. Sci.*, 71, 150–167,
851 doi:10.1016/j.jes.2017.12.017, 2018.

852 Chowdhury, Z., Zheng, M., Cass, G. R., Sheesley, R. J., Schauer, J. J., Salmon, L. G. and Russell, A. G.:
853 Source apportionment and characterization of ambient fine particles in Delhi, in *Symposium on Air
854 Quality Measurement Methods and Technology 2004*, pp. 13–24., 2004.

855 Coggon, M. M., Gkatzelis, G. I., McDonald, B. C., Gilman, J. B., Schwantes, R. H., Abuhassan, N.,
856 Aikin, K. C., Arendt, M. F., Berkoff, T. A., Brown, S. S., Campos, T. L., Dickerson, R. R., Gronoff, G.,
857 Hurley, J. F., Isaacman-Vanwertz, G., Koss, A. R., Li, M., McKeen, S. A., Moshary, F., Peischl, J.,
858 Pospisilova, V., Ren, X., Wilson, A., Wu, Y., Trainer, M. and Warneke, C.: Volatile chemical product
859 emissions enhance ozone and modulate urban chemistry, *Proc. Natl. Acad. Sci. U. S. A.*, 118(32),
860 e2026653118, doi:10.1073/PNAS.2026653118/SUPPL_FILE/PNAS.2026653118.SAPP.PDF, 2021.

861 Darer, A. I., Cole-Filipiak, N. C., O'Connor, A. E. and Elrod, M. J.: Formation and stability of
862 atmospherically relevant isoprene-derived organosulfates and organonitrates, *Environ. Sci. Technol.*,
863 45(5), 1895–1902, doi:10.1021/es103797z, 2011.

864 Ding, J., Zhao, P., Su, J., Dong, Q., Du, X. and Zhang, Y.: Aerosol pH and its driving factors in Beijing,
865 *Atmos. Chem. Phys.*, 19(12), 7939–7954, doi:10.5194/ACP-19-7939-2019, 2019.

866 Drozd, G. T., Woo, J. L. and McNeill, V. F.: Self-limited uptake of α -pinene oxide to acidic aerosol: The
867 effects of liquid-liquid phase separation and implications for the formation of secondary organic
868 aerosol and organosulfates from epoxides, *Atmos. Chem. Phys.*, 13(16), 8255–8263,
869 doi:10.5194/acp-13-8255-2013, 2013.

870 Du, Z., He, K., Cheng, Y., Duan, F., Ma, Y., Liu, J., Zhang, X., Zheng, M. and Weber, R.: A yearlong study
871 of water-soluble organic carbon in Beijing I: Sources and its primary vs. secondary nature, *Atmos.*
872 *Environ.*, 92, 514–521, doi:10.1016/j.atmosenv.2014.04.060, 2014.

873 Eddingsaas, N. C., Loza, C. L., Yee, L. D., Seinfeld, J. H. and Wennberg, P. O.: α -pinene photooxidation
874 under controlled chemical conditions-Part 1: Gas-phase composition in low-and high-NO
875 xenvironments, *Atmos. Chem. Phys.*, 12(14), 6489–6504, doi:10.5194/acp-12-6489-2012, 2012a.

876 Eddingsaas, N. C., Loza, C. L., Yee, L. D., Chan, M., Schilling, K. A., Chhabra, P. S., Seinfeld, J. H. and
877 Wennberg, P. O.: α -pinene photooxidation under controlled chemical conditions-Part 2: SOA yield

878 and composition in low-and high-NO_x environments, *Atmos. Chem. Phys.*, 12(16), 7413–7427,
879 doi:10.5194/acp-12-7413-2012, 2012b.

880 Elser, M., Huang, R. J., Wolf, R., Slowik, J. G., Wang, Q., Canonaco, F., Li, G., Bozzetti, C., Daellenbach,
881 K. R., Huang, Y., Zhang, R., Li, Z., Cao, J., Baltensperger, U., El-Haddad, I. and André, P.: New insights
882 into PM_{2.5} chemical composition and sources in two major cities in China during extreme haze
883 events using aerosol mass spectrometry, *Atmos. Chem. Phys.*, 16(5), 3207–3225, doi:10.5194/ACP-
884 16-3207-2016, 2016.

885 Elzein, A., Stewart, G. J., Swift, S. J., Nelson, B. S., Crilley, L. R., Alam, M. S., Reyes-Villegas, E., Gadi,
886 R., Harrison, R. M., Hamilton, J. F. and Lewis, A. C.: A comparison of PM_{2.5}-bound polycyclic
887 aromatic hydrocarbons in summer Beijing (China) and Delhi (India), *Atmos. Chem. Phys.*, 20(22),
888 14303–14319, doi:10.5194/ACP-20-14303-2020, 2020.

889 Galloway, M. M., Chhabra, P. S., Chan, A. W. H., Surratt, J. D., Flagan, R. C., Seinfeld, J. H. and
890 Keutsch, F. N.: Glyoxal uptake on ammonium sulphate seed aerosol: Reaction products and
891 reversibility of uptake under dark and irradiated conditions, *Atmos. Chem. Phys.*, 9(10), 3331–3345,
892 doi:10.5194/acp-9-3331-2009, 2009.

893 Gani, S., Bhandari, S., Seraj, S., Wang, D. S., Patel, K., Soni, P., Arub, Z., Habib, G., Hildebrandt Ruiz, L.
894 and Apte, J. S.: Submicron aerosol composition in the world's most polluted megacity: the Delhi
895 Aerosol Supersite study, *Atmos. Chem. Phys.*, 19(10), 6843–6859, doi:10.5194/acp-19-6843-2019,
896 2019.

897 Gaston, C. J., Riedel, T. P., Zhang, Z., Gold, A., Surratt, J. D. and Thornton, J. A.: Reactive Uptake of an
898 Isoprene-Derived Epoxydiol to Submicron Aerosol Particles, *Environ. Sci. Technol.*, 48(19), 11178–
899 11186, doi:10.1021/es5034266, 2014.

900 Gkatzelis, G. I., Coggon, M. M., McDonald, B. C., Peischl, J., Gilman, J. B., Aikin, K. C., Robinson, M. A.,
901 Canonaco, F., Prevot, A. S. H., Trainer, M. and Warneke, C.: Observations Confirm that Volatile
902 Chemical Products Are a Major Source of Petrochemical Emissions in U.S. Cities, *Environ. Sci.*
903 *Technol.*, 55(8), 4332–4343, doi:10.1021/ACS.EST.0C05471/SUPPL_FILE/ES0C05471_SI_001.PDF,
904 2021.

905 Glasius, M., Bering, M. S., Yee, L. D., de Sá, S. S., Isaacman-VanWertz, G., Wernis, R. A., Barbosa, H.
906 M. J., Alexander, M. L., Palm, B. B., Hu, W., Campuzano-Jost, P., Day, D. A., Jimenez, J. L., Shrivastava,
907 M., Martin, S. T. and Goldstein, A. H.: Organosulfates in aerosols downwind of an urban region in
908 central Amazon, *Environ. Sci. Process. Impacts*, 20(11), 1546–1558, doi:10.1039/C8EM00413G, 2018.

909 Guenther, A. B., Jiang, X., Heald, C. L., Sakulyanontvittaya, T., Duhl, T., Emmons, L. K. and Wang, X.:
910 The Model of Emissions of Gases and Aerosols from Nature version 2.1 (MEGAN2.1): an extended
911 and updated framework for modeling biogenic emissions, *Geosci. Model Dev.*, 5(6), 1471–1492,
912 doi:10.5194/gmd-5-1471-2012, 2012.

913 Hallquist, M., Wenger, J. C., Baltensperger, U., Rudich, Y., Simpson, D., Claeys, M., Dommen, J.,
914 Donahue, N. M., George, C., Goldstein, A. H., Hamilton, J. F., Herrmann, H., Hoffmann, T., Iinuma, Y.,
915 Jang, M., Jenkin, M. E., Jimenez, J. L., Kiendler-Scharr, A., Maenhaut, W., McFiggans, G., Mentel, T. F.,
916 Monod, A., Prévôt, A. S. H., Seinfeld, J. H., Surratt, J. D., Szmigielski, R. and Wildt, J.: The formation,
917 properties and impact of secondary organic aerosol: current and emerging issues, *Atmos. Chem.*
918 *Phys.*, 9(14), 5155–5236, doi:10.5194/acp-9-5155-2009, 2009.

919 Hama, S. M. L., Kumar, P., Harrison, R. M., Bloss, W. J., Khare, M., Mishra, S., Namdeo, A., Sokhi, R.,
920 Goodman, P. and Sharma, C.: Four-year assessment of ambient particulate matter and trace gases in
921 the Delhi-NCR region of India, *Sustain. Cities Soc.*, 54, doi:10.1016/j.scs.2019.102003, 2020.

922 Hamilton, J. F., Bryant, D. J., Edwards, P. M., Ouyang, B., Bannan, T. J., Mehra, A., Mayhew, A. W.,

923 Hopkins, J. R., Dunmore, R. E., Squires, F. A., Lee, J. D., Newland, M. J., Worrall, S. D., Bacak, A., Coe,
924 H., Whalley, L. K., Heard, D. E., Slater, E. J., Jones, R. L., Cui, T., Surratt, J. D., Reeves, C. E., Mills, G. P.,
925 Grimmond, S., Sun, Y., Xu, W., Shi, Z. and Rickard, A. R.: Key Role of NO₃ Radicals in the Production
926 of Isoprene Nitrates and Nitrooxyorganosulfates in Beijing, *Environ. Sci. Technol.*, 55(2), 842–853,
927 doi:10.1021/acs.est.0c05689, 2021.

928 Hatch, L. E., Jen, C. N., Kreisberg, N. M., Selimovic, V., Yokelson, R. J., Stamatis, C., York, R. A., Foster,
929 D., Stephens, S. L., Goldstein, A. H. and Barsanti, K. C.: Highly Speciated Measurements of Terpenoids
930 Emitted from Laboratory and Mixed-Conifer Forest Prescribed Fires, *Environ. Sci. Technol.*, 53(16),
931 9418–9428, doi:10.1021/ACS.EST.9B02612, 2019.

932 Hettiyadura, A. P. S., Al-Naiema, I. M., Hughes, D. D., Fang, T. and Stone, E. A.: Organosulfates in
933 Atlanta, Georgia: anthropogenic influences on biogenic secondary organic aerosol formation, *Atmos.*
934 *Chem. Phys.*, 19(5), 3191–3206, doi:10.5194/acp-19-3191-2019, 2019.

935 Hoffmann, T., Odum, J. R., Bowman, F., Collins, D., Klockow, D., Flagan, R. C. and Seinfeld, J. H.:
936 Formation of organic aerosols from the oxidation of biogenic hydrocarbons, *J. Atmos. Chem.*, 26(2),
937 189–222, doi:10.1023/A:1005734301837, 1997.

938 Hoyle, C. R., Boy, M., Donahue, N. M., Fry, J. L., Glasius, M., Guenther, A., Hallar, A. G., Huff Hartz, K.,
939 Petters, M. D., Petäjä, T., Rosenoern, T. and Sullivan, A. P.: A review of the anthropogenic influence
940 on biogenic secondary organic aerosol, *Atmos. Chem. Phys.*, 11(1), 321–343, doi:10.5194/acp-11-
941 321-2011, 2011.

942 Hsieh, H.-C., Ou-Yang, C.-F. and Wang, J.-L.: Revelation of Coupling Biogenic with Anthropogenic
943 Isoprene by Highly Time-Resolved Observations, *Aerosol Air Qual. Res.*, 17(3), 721–729,
944 doi:10.4209/AAQR.2016.04.0133, 2017.

945 Hu, W., Hu, M., Hu, W., Jimenez, J. L., Yuan, B., Chen, W., Wang, M., Wu, Y., Chen, C., Wang, Z., Peng,
946 J., Zeng, L. and Shao, M.: Chemical composition, sources, and aging process of submicron aerosols in
947 Beijing: Contrast between summer and winter, *J. Geophys. Res. Atmos.*, 121(4), 1955–1977,
948 doi:10.1002/2015JD024020, 2016.

949 Huang, Z., Zhang, Y., Yan, Q., Zhang, Z. and Wang, X.: Real-time monitoring of respiratory absorption
950 factors of volatile organic compounds in ambient air by proton transfer reaction time-of-flight mass
951 spectrometry, *J. Hazard. Mater.*, 320, 547–555, doi:10.1016/J.JHAZMAT.2016.08.064, 2016.

952 Iinuma, Y., Müller, C., Berndt, T., Böge, O., Claeys, M. and Herrmann, H.: Evidence for the existence
953 of organosulfates from β -pinene ozonolysis in ambient secondary organic aerosol, *Environ. Sci.*
954 *Technol.*, 41(19), 6678–6683, doi:10.1021/es070938t, 2007.

955 Jain, N., Bhatia, A. and Pathak, H.: Emission of Air Pollutants from Crop Residue Burning in India,
956 *Aerosol Air Qual. Res.*, 14(1), 422–430, doi:10.4209/aaqr.2013.01.0031, 2014.

957 Javed, M., Bashir, M. and Zaineb, S.: Analysis of daily and seasonal variation of fine particulate
958 matter (PM_{2.5}) for five cities of China, *Environ. Dev. Sustain.*, 1–29, doi:10.1007/s10668-020-01159-
959 1, 2021.

960 Kanawade, V. P., Srivastava, A. K., Ram, K., Asmi, E., Vakkari, V., Soni, V. K., Varaprasad, V. and
961 Sarangi, C.: What caused severe air pollution episode of November 2016 in New Delhi?, *Atmos.*
962 *Environ.*, 222, doi:10.1016/j.atmosenv.2019.117125, 2020.

963 Kashyap, P., Kumar, A., Kumar, R. P. and Kumar, K.: Biogenic and anthropogenic isoprene emissions
964 in the subtropical urban atmosphere of Delhi, *Atmos. Pollut. Res.*, 10(5), 1691–1698,
965 doi:10.1016/j.apr.2019.07.004, 2019.

966 Khan, M. A. H., Schlich, B.-L., Jenkin, M. E., Shallcross, B. M. A., Moseley, K., Walker, C., Morris, W. C.,

967 Derwent, R. G., Percival, C. J. and Shallcross, D. E.: A Two-Decade Anthropogenic and Biogenic
968 Isoprene Emissions Study in a London Urban Background and a London Urban Traffic Site, *Atmos.*
969 2018, Vol. 9, Page 387, 9(10), 387, doi:10.3390/ATMOS9100387, 2018a.

970 Khan, M. A. H., Schlich, B. L., Jenkin, M. E., Shallcross, B. M. A., Moseley, K., Walker, C., Morris, W. C.,
971 Derwent, R. G., Percival, C. J. and Shallcross, D. E.: A Two-Decade Anthropogenic and Biogenic
972 Isoprene Emissions Study in a London Urban Background and a London Urban Traffic Site, *Atmos.*
973 2018, Vol. 9, Page 387, 9(10), 387, doi:10.3390/ATMOS9100387, 2018b.

974 Kirillova, E. N., Sheesley, R. J., Andersson, A. and Gustafsson, Ö.: Natural abundance ¹³C and ¹⁴C
975 analysis of water-soluble organic carbon in atmospheric aerosols, *Anal. Chem.*, 82(19), 7973–7978,
976 doi:10.1021/ac1014436, 2010.

977 Kirillova, E. N., Andersson, A., Sheesley, R. J., Kruså, M., Praveen, P. S., Budhavant, K., Safai, P. D.,
978 Rao, P. S. P. and Gustafsson, Ö.: ¹³C- and ¹⁴C-based study of sources and atmospheric processing of
979 water-soluble organic carbon (WSOC) in South Asian aerosols, *J. Geophys. Res. Atmos.*, 118(2), 614–
980 626, doi:10.1002/jgrd.50130, 2013.

981 Kirillova, E. N., Andersson, A., Tiwari, S., Srivastava, A. K., Bisht, D. S. and Gustafsson, Ö.: Water-
982 soluble organic carbon aerosols during a full New Delhi winter: Isotope-based source apportionment
983 and optical properties, *J. Geophys. Res. Atmos.*, 119(6), 3476–3485, doi:10.1002/2013JD020041,
984 2014.

985 Klein, F., Farren, N. J., Bozzetti, C., Daellenbach, K. R., Kilic, D., Kumar, N. K., Pieber, S. M., Slowik, J.
986 G., Tuthill, R. N., Hamilton, J. F., Baltensperger, U., Prévôt, A. S. H. and El Haddad, I.: Indoor terpene
987 emissions from cooking with herbs and pepper and their secondary organic aerosol production
988 potential, *Sci. Reports* 2016 61, 6(1), 1–7, doi:10.1038/srep36623, 2016.

989 Kleindienst, T. E., Edney, E. O., Lewandowski, M., Offenber, J. H. and Jaoui, M.: Secondary Organic
990 Carbon and Aerosol Yields from the Irradiations of Isoprene and α -Pinene in the Presence of NO_x
991 and SO₂, *Environ. Sci. Technol.*, 40(12), 3807–3812, doi:10.1021/es052446r, 2006.

992 Kourtchev, I., Godoi, R. H. M., Connors, S., Levine, J. G., Archibald, A. T., Godoi, A. F. L., Paralovo, S.
993 L., Barbosa, C. G. G., Souza, R. A. F., Manzi, A. O., Seco, R., Sjostedt, S., Park, J. H., Guenther, A., Kim,
994 S., Smith, J., Martin, S. T. and Kalberer, M.: Molecular composition of organic aerosols in central
995 Amazonia: An ultra-high-resolution mass spectrometry study, *Atmos. Chem. Phys.*, 16(18), 11899–
996 11913, doi:10.5194/acp-16-11899-2016, 2016.

997 Kristensen, K., Enggrob, K. L., King, S. M., Worton, D. R., Platt, S. M., Mortensen, R., Rosenoern, T.,
998 Surratt, J. D., Bilde, M., Goldstein, A. H. and Glasius, M.: Formation and occurrence of dimer esters of
999 pinene oxidation products in atmospheric aerosols, *Atmos. Chem. Phys.*, 13(7), 3763–3776,
1000 doi:10.5194/acp-13-3763-2013, 2013.

1001 Kumar, P., Kumar, S. and Yadav, S.: Seasonal variations in size distribution, water-soluble ions, and
1002 carbon content of size-segregated aerosols over New Delhi, *Environ. Sci. Pollut. Res.*, 25(6), 6061–
1003 6078, doi:10.1007/S11356-017-0954-6, 2018.

1004 Landrigan, P. J., Fuller, R., Acosta, N. J. R., Adayi, O., Arnold, R., Basu, N. (Nil), Baldé, A. B., Bertollini,
1005 R., Bose-O'Reilly, S., Boufford, J. I., Breyse, P. N., Chiles, T., Mahidol, C., Coll-Seck, A. M., Cropper, M.
1006 L., Fobil, J., Fuster, V., Greenstone, M., Haines, A., Hanrahan, D., Hunter, D., Khare, M., Krupnick, A.,
1007 Lanphear, B., Lohani, B., Martin, K., Mathiasen, K. V., McTeer, M. A., Murray, C. J. L., Ndahimananjara,
1008 J. D., Perera, F., Potočník, J., Preker, A. S., Ramesh, J., Rockström, J., Salinas, C., Samson, L. D.,
1009 Sandilya, K., Sly, P. D., Smith, K. R., Steiner, A., Stewart, R. B., Suk, W. A., van Schayck, O. C. P.,
1010 Yadama, G. N., Yumkella, K. and Zhong, M.: The Lancet Commission on pollution and health, *Lancet*,
1011 391(10119), 462–512, doi:10.1016/S0140-6736(17)32345-0, 2018.

1012 Lanz, V. A., Přeřot, A. S. H., Alfarra, M. R., Weimer, S., Mohr, C., Decarlo, P. F., Gianini, M. F. D.,
1013 Hueglin, C., Schneider, J., Favez, O., D'Anna, B., George, C. and Baltensperger, U.: Characterization of
1014 aerosol chemical composition with aerosol mass spectrometry in Central Europe: An overview,
1015 *Atmos. Chem. Phys.*, 10(21), 10453–10471, doi:10.5194/ACP-10-10453-2010, 2010.

1016 Lee, B. H., Mohr, C., Lopez-Hilfiker, F. D., Lutz, A., Hallquist, M., Lee, L., Romer, P., Cohen, R. C., Iyer,
1017 S., Kurtén, T., Hu, W., Day, D. A., Campuzano-Jost, P., Jimenez, J. L., Xu, L., Ng, N. L., Guo, H., Weber,
1018 R. J., Wild, R. J., Brown, S. S., Koss, A., de Gouw, J., Olson, K., Goldstein, A. H., Seco, R., Kim, S.,
1019 McAvey, K., Shepson, P. B., Starn, T., Baumann, K., Edgerton, E. S., Liu, J., Shilling, J. E., Miller, D. O.,
1020 Brune, W., Schobesberger, S., D'Ambro, E. L. and Thornton, J. A.: Highly functionalized organic
1021 nitrates in the southeast United States: Contribution to secondary organic aerosol and reactive
1022 nitrogen budgets., *Proc. Natl. Acad. Sci. U. S. A.*, 113(6), 1516–21, doi:10.1073/pnas.1508108113,
1023 2016.

1024 Lelieveld, J., Gromov, S., Pozzer, A. and Taraborrelli, D.: Global tropospheric hydroxyl distribution,
1025 budget and reactivity, *Atmos. Chem. Phys.*, 16(19), 12477–12493, doi:10.5194/ACP-16-12477-2016,
1026 2016.

1027 Liao, J., Froyd, K. D., Murphy, D. M., Keutsch, F. N., Yu, G., Wennberg, P. O., St. Clair, J. M., Crounse,
1028 J. D., Wisthaler, A., Mikoviny, T., Jimenez, J. L., Campuzano-Jost, P., Day, D. A., Hu, W., Ryerson, T. B.,
1029 Pollack, I. B., Peischl, J., Anderson, B. E., Ziemba, L. D., Blake, D. R., Meinardi, S. and Diskin, G.:
1030 Airborne measurements of organosulfates over the continental U.S., *J. Geophys. Res.*, 120(7), 2990–
1031 3005, doi:10.1002/2014JD022378, 2015.

1032 Lin, Y. H., Zhang, Z., Docherty, K. S., Zhang, H., Budisulistiorini, S. H., Rubitschun, C. L., Shaw, S. L.,
1033 Knipping, E. M., Edgerton, E. S., Kleindienst, T. E., Gold, A. and Surratt, J. D.: Isoprene epoxydiols as
1034 precursors to secondary organic aerosol formation: Acid-catalyzed reactive uptake studies with
1035 authentic compounds, *Environ. Sci. Technol.*, 46(1), 250–258, doi:10.1021/es202554c, 2012.

1036 Lin, Y. H., Zhang, H., Pye, H. O. T., Zhang, Z., Marth, W. J., Park, S., Arashiro, M., Cui, T.,
1037 Budisulistiorini, S. H., Sexton, K. G., Vizuete, W., Xie, Y., Luecken, D. J., Piletic, I. R., Edney, E. O.,
1038 Bartolotti, L. J., Gold, A. and Surratt, J. D.: Epoxide as a precursor to secondary organic aerosol
1039 formation from isoprene photooxidation in the presence of nitrogen oxides, *Proc. Natl. Acad. Sci. U.*
1040 *S. A.*, 110(17), 6718–6723, doi:10.1073/pnas.1221150110, 2013a.

1041 Lin, Y. H., Knipping, E. M., Edgerton, E. S., Shaw, S. L. and Surratt, J. D.: Investigating the influences of
1042 SO₂ and NH₃ levels on isoprene-derived secondary organic aerosol formation using conditional
1043 sampling approaches, *Atmos. Chem. Phys.*, 13(16), 8457–8470, doi:10.5194/ACP-13-8457-2013,
1044 2013b.

1045 Lin, Y. H., Budisulistiorini, S. H., Chu, K., Siejack, R. A., Zhang, H., Riva, M., Zhang, Z., Gold, A.,
1046 Kautzman, K. E. and Surratt, J. D.: Light-absorbing oligomer formation in secondary organic aerosol
1047 from reactive uptake of isoprene epoxydiols, *Environ. Sci. Technol.*, 48(20), 12012–12021,
1048 doi:10.1021/es503142b, 2014.

1049 Mishra, A. K. and Sinha, V.: Emission drivers and variability of ambient isoprene, formaldehyde and
1050 acetaldehyde in north-west India during monsoon season, *Environ. Pollut.*, 267, 115538,
1051 doi:10.1016/J.ENVPOL.2020.115538, 2020.

1052 Miyazaki, Y., Aggarwal, S. G., Singh, K., Gupta, P. K. and Kawamura, K.: Dicarboxylic acids and water-
1053 soluble organic carbon in aerosols in New Delhi, India, in winter: Characteristics and formation
1054 processes, *J. Geophys. Res. Atmos.*, 114(19), doi:10.1029/2009JD011790, 2009.

1055 Morales, A. C., Jayarathne, T., Slade, J. H., Laskin, A. and Shepson, P. B.: The production and
1056 hydrolysis of organic nitrates from OH radical oxidation of β -ocimene, *Atmos. Chem. Phys.*, 21(1),
1057 129–145, doi:10.5194/ACP-21-129-2021, 2021.

1058 Mutzel, A., Rodigast, M., Iinuma, Y., Böge, O. and Herrmann, H.: Monoterpene SOA - Contribution of
1059 first-generation oxidation products to formation and chemical composition, *Atmos. Environ.*, **130**,
1060 136–144, doi:10.1016/j.atmosenv.2015.10.080, 2016.

1061 Nagar, P. K., Singh, D., Sharma, M., Kumar, A., Aneja, V. P., George, M. P., Agarwal, N. and Shukla, S.
1062 P.: Characterization of PM_{2.5} in Delhi: role and impact of secondary aerosol, burning of biomass, and
1063 municipal solid waste and crustal matter, *Environ. Sci. Pollut. Res.*, **24**(32), 25179–25189,
1064 doi:10.1007/s11356-017-0171-3, 2017.

1065 Nelson, B., Stewart, G., Drysdale, W., Newland, M., Vaughan, A., Dunmore, R., Edwards, P., Lewis, A.,
1066 Hamilton, J., Acton, W. J. F., Hewitt, C. N., Crilley, L., Alam, M., Şahin, Ü., Beddows, D., Bloss, W.,
1067 Slater, E., Whalley, L., Heard, D., Cash, J., Langford, B., Nemitz, E., Sommariva, R., Cox, S., Gadi, R.,
1068 Gurjar, B., Hopkins, J., Rickard, A. and Lee, J.: In situ Ozone Production is highly sensitive to Volatile
1069 Organic Compounds in the Indian Megacity of Delhi, *Atmos. Chem. Phys. Discuss.*, 1–36,
1070 doi:10.5194/ACP-2021-278, 2021.

1071 Nestorowicz, K., Jaoui, M., Rudzinski, K. J., Lewandowski, M., Kleindienst, T. E., Spólnik, G.,
1072 Danikiewicz, W. and Szmigielski, R.: Chemical composition of isoprene SOA under acidic and non-
1073 acidic conditions: effect of relative humidity, *Atmos. Chem. Phys.*, **18**(24), 18101–18121,
1074 doi:10.5194/acp-18-18101-2018, 2018.

1075 Newland, M. J., Bryant, D. J., Dunmore, R. E., Bannan, T. J., Joe, W., Langford, B., Hopkins, J. R.,
1076 Squires, F. A., Dixon, W., Drysdale, W. S., Ivatt, P. D., Evans, M. J., Edwards, P. M., Whalley, L. K.,
1077 Heard, D. E., Slater, E. J., Woodward-Massey, R., Ye, C., Mehra, A., Worrall, S. D., Bacak, A., Coe, H.,
1078 Percival, C. J., Nicholas Hewitt, C., Lee, J. D., Cui, T., Surratt, J. D., Wang, X., Lewis, A. C., Rickard, A. R.
1079 and Hamilton, J. F.: Low-NO atmospheric oxidation pathways in a polluted megacity, *Atmos. Chem.
1080 Phys.*, **21**(3), 1613–1625, doi:10.5194/acp-21-1613-2021, 2021.

1081 Ng, N. L., Kwan, A. J., Surratt, J. D., Chan, A. W. H., Chhabra, P. S., Sorooshian, A., Pye, H. O. T.,
1082 Crouse, J. D., Wennberg, P. O., Flagan, R. C. and Seinfeld, J. H.: Secondary organic aerosol (SOA)
1083 formation from reaction of isoprene with nitrate radicals (NO₃), *Atmos. Chem. Phys.*, **8**(14), 4117–
1084 4140, doi:10.5194/acp-8-4117-2008, 2008.

1085 Ng, N. L., Brown, S. S., Archibald, A. T., Atlas, E., Cohen, R. C., Crowley, J. N., Day, D. A., Donahue, N.
1086 M., Fry, J. L., Fuchs, H., Griffin, R. J., Guzman, M. I., Herrmann, H., Hodzic, A., Iinuma, Y., Jimenez, J.
1087 L., Kiendler-Scharr, A., Lee, B. H., Luecken, D. J., Mao, J., McLaren, R., Mutzel, A., Osthoff, H. D.,
1088 Ouyang, B., Picquet-Varrault, B., Platt, U., Pye, H. O. T., Rudich, Y., Schwantes, R. H., Shiraiwa, M.,
1089 Stutz, J., Thornton, J. A., Tilgner, A., Williams, B. J. and Zaveri, R. A.: Nitrate radicals and biogenic
1090 volatile organic compounds: oxidation, mechanisms, and organic aerosol, *Atmos. Chem. Phys.*, **17**(3),
1091 2103–2162, doi:10.5194/acp-17-2103-2017, 2017.

1092 Nguyen, Q. T., Christensen, M. K., Cozzi, F., Zare, A., Hansen, A. M. K., Kristensen, K., Tulinius, T. E.,
1093 Madsen, H. H., Christensen, J. H., Brandt, J., Massling, A., Nøjgaard, J. K. and Glasius, M.:
1094 Understanding the anthropogenic influence on formation of biogenic secondary organic aerosols in
1095 Denmark via analysis of organosulfates and related oxidation products, *Atmos. Chem. Phys.*, **14**(17),
1096 8961–8981, doi:10.5194/acp-14-8961-2014, 2014.

1097 Nguyen, T. B., Bateman, A. P., Bones, D. L., Nizkorodov, S. A., Laskin, J. and Laskin, A.: High-resolution
1098 mass spectrometry analysis of secondary organic aerosol generated by ozonolysis of isoprene,
1099 *Atmos. Environ.*, **44**(8), 1032–1042, doi:10.1016/J.ATMOSENV.2009.12.019, 2010.

1100 Nguyen, T. B., Bates, K. H., Crouse, J. D., Schwantes, R. H., Zhang, X., Kjaergaard, H. G., Surratt, J. D.,
1101 Lin, P., Laskin, A., Seinfeld, J. H. and Wennberg, P. O.: Mechanism of the hydroxyl radical oxidation of
1102 methacryloyl peroxyxynitrate (MPAN) and its pathway toward secondary organic aerosol formation in
1103 the atmosphere, *Phys. Chem. Chem. Phys.*, **17**(27), 17914–17926, doi:10.1039/c5cp02001h, 2015.

1104 None, S., R, G., SK, S. and TK, M.: Seasonal variation, source apportionment and source attributed
1105 health risk of fine carbonaceous aerosols over National Capital Region, India, *Chemosphere*, 237,
1106 doi:10.1016/J.CHEMOSPHERE.2019.124500, 2019.

1107 Panopoulou, A., Liakakou, E., Sauvage, S., Gros, V., Locoge, N., Stavroulas, I., Bonsang, B.,
1108 Gerasopoulos, E. and Mihalopoulos, N.: Yearlong measurements of monoterpenes and isoprene in a
1109 Mediterranean city (Athens): Natural vs anthropogenic origin, *Atmos. Environ.*, 243, 117803,
1110 doi:10.1016/J.ATMOSENV.2020.117803, 2020.

1111 Panopoulou, A., Liakakou, E., Sauvage, S., Gros, V., Locoge, N., Bonsang, B., Salameh, T.,
1112 Gerasopoulos, E. and Mihalopoulos, N.: Variability and sources of non-methane hydrocarbons at a
1113 Mediterranean urban atmosphere: The role of biomass burning and traffic emissions, *Sci. Total*
1114 *Environ.*, 800, 149389, doi:10.1016/J.SCITOTENV.2021.149389, 2021.

1115 Passananti, M., Kong, L., Shang, J., Dupart, Y., Perrier, S., Chen, J., Donaldson, D. J. and George, C.:
1116 Organosulfate Formation through the Heterogeneous Reaction of Sulfur Dioxide with Unsaturated
1117 Fatty Acids and Long-Chain Alkenes, *Angew. Chemie - Int. Ed.*, 55(35), 10336–10339,
1118 doi:10.1002/anie.201605266, 2016.

1119 Paulot, F., Crouse, J. D., Kjaergaard, H. G., Kurten, A., St. Clair, J. M., Seinfeld, J. H. and Wennberg, P.
1120 O.: Unexpected Epoxide Formation in the Gas-Phase Photooxidation of Isoprene, *Science (80-.)*,
1121 325(5941), 730–733, doi:10.1126/science.1172910, 2009.

1122 Rattanavaraha, W., Chu, K., Budisulistiorini, S. H., Riva, M., Lin, Y.-H., Edgerton, E. S., Baumann, K.,
1123 Shaw, S. L., Guo, H., King, L., Weber, R. J., Neff, M. E., Stone, E. A., Offenberg, J. H., Zhang, Z., Gold, A.
1124 and Surratt, J. D.: Assessing the impact of anthropogenic pollution on isoprene-derived secondary
1125 organic aerosol formation in PM_{2.5} collected from the Birmingham, Alabama, ground site during the
1126 Birmingham, Alabama, ground site during the 2013 Southern Oxidant and Aerosol Study, *Atmos.*
1127 *Chem. Phys.*, 16(8), 4897–4914, doi:10.5194/acp-16-4897-2016, 2016a.

1128 Rattanavaraha, W., Chu, K., Budisulistiorini, S. H., Riva, M., Lin, Y. H., Edgerton, E. S., Baumann, K.,
1129 Shaw, S. L., Guo, H., King, L., Weber, R. J., Neff, M. E., Stone, E. A., Offenberg, J. H., Zhang, Z., Gold, A.
1130 and Surratt, J. D.: Assessing the impact of anthropogenic pollution on isoprene-derived secondary
1131 organic aerosol formation in PM_{2.5} collected from the Birmingham, Alabama, ground site during the
1132 2013 Southern Oxidant and Aerosol Study, *Atmos. Chem. Phys.*, 16(8), 4897–4914, doi:10.5194/acp-
1133 16-4897-2016, 2016b.

1134 Reyes-Villegas, E., Panda, U., Darbyshire, E., Cash, J. M., Joshi, R., Langford, B., Di Marco, C. F.,
1135 Mullinger, N. J., Alam, M. S., Crilley, L. R., Rooney, D. J., Acton, W. J. F., Drysdale, W., Nemitz, E.,
1136 Flynn, M., Voliotis, A., McFiggans, G., Coe, H., Lee, J., Hewitt, C. N., Heal, M. R., Gunthe, S. S., Mandal,
1137 T. K., Gurjar, B. R., Shivani, Gadi, R., Singh, S., Soni, V. and Allan, J. D.: PM₁ composition and source
1138 apportionment at two sites in Delhi, India, across multiple seasons, *Atmos. Chem. Phys.*, 21(15),
1139 11655–11667, doi:10.5194/ACP-21-11655-2021, 2021.

1140 Riva, M., Da Silva Barbosa, T., Lin, Y.-H., Stone, E. A., Gold, A. and Surratt, J. D.: Chemical
1141 characterization of organosulfates in secondary organic aerosol derived from the photooxidation of
1142 alkanes, *Atmos. Chem. Phys.*, 16(17), 11001–11018, doi:10.5194/acp-16-11001-2016, 2016a.

1143 Riva, M., Budisulistiorini, S. H., Zhang, Z. and Gold, A.: Chemical characterization of secondary
1144 organic aerosol constituents from isoprene ozonolysis in the presence of acidic aerosol, *Atmos.*
1145 *Environ.*, 130, 5–13, doi:10.1016/J.ATMOSENV.2015.06.027, 2016b.

1146 Riva, M., Bell, D. M., Hansen, A. M. K., Drozd, G. T., Zhang, Z., Gold, A., Imre, D., Surratt, J. D., Glasius,
1147 M. and Zelenyuk, A.: Effect of Organic Coatings, Humidity and Aerosol Acidity on Multiphase
1148 Chemistry of Isoprene Epoxidiols, *Environ. Sci. Technol.*, 50(11), 5580–5588,
1149 doi:10.1021/acs.est.5b06050, 2016c.

1150 Riva, M., Chen, Y., Zhang, Y., Lei, Z., Olson, N. E., Boyer, H. C., Narayan, S., Yee, L. D., Green, H. S., Cui,
1151 T., Zhang, Z., Baumann, K., Fort, M., Edgerton, E., Budisulistiorini, S. H., Rose, C. A., Ribeiro, I. O., e
1152 Oliveira, R. L., dos Santos, E. O., Machado, C. M. D., Szopa, S., Zhao, Y., Alves, E. G., de Sá, S. S., Hu,
1153 W., Knipping, E. M., Shaw, S. L., Duvoisin Junior, S., de Souza, R. A. F., Palm, B. B., Jimenez, J.-L.,
1154 Glasius, M., Goldstein, A. H., Pye, H. O. T., Gold, A., Turpin, B. J., Vizuete, W., Martin, S. T., Thornton,
1155 J. A., Dutcher, C. S., Ault, A. P. and Surratt, J. D.: Increasing Isoprene Epoxydiol-to-Inorganic Sulfate
1156 Aerosol Ratio Results in Extensive Conversion of Inorganic Sulfate to Organosulfur Forms:
1157 Implications for Aerosol Physicochemical Properties, *Environ. Sci. Technol.*, acs.est.9b01019,
1158 doi:10.1021/acs.est.9b01019, 2019.

1159 Saha, D., Soni, K., Mohanan, M. N. and Singh, M.: Long-term trend of ventilation coefficient over
1160 Delhi and its potential impacts on air quality, *Remote Sens. Appl. Soc. Environ.*, 15, 100234,
1161 doi:10.1016/J.RSASE.2019.05.003, 2019.

1162 Sahu, L. K. and Saxena, P.: High time and mass resolved PTR-TOF-MS measurements of VOCs at an
1163 urban site of India during winter: Role of anthropogenic, biomass burning, biogenic and
1164 photochemical sources, *Atmos. Res.*, 164–165, 84–94, doi:10.1016/J.ATMOSRES.2015.04.021, 2015.

1165 Sahu, L. K., Tripathi, N. and Yadav, R.: Contribution of biogenic and photochemical sources to
1166 ambient VOCs during winter to summer transition at a semi-arid urban site in India, *Environ. Pollut.*,
1167 229, 595–606, doi:10.1016/J.ENVPOL.2017.06.091, 2017.

1168 Sawlani, R., Agnihotri, R., Sharma, C., Patra, P. K., Dimri, A. P., Ram, K. and Verma, R. L.: The severe
1169 Delhi SMOG of 2016: A case of delayed crop residue burning, coincident firecracker emissions, and
1170 atypical meteorology, *Atmos. Pollut. Res.*, 10(3), 868–879, doi:10.1016/j.apr.2018.12.015, 2019.

1171 Schindelka, J., Iinuma, Y., Hoffmann, D. and Herrmann, H.: Sulfate radical-initiated formation of
1172 isoprene-derived organosulfates in atmospheric aerosols, *Faraday Discuss.*, 165(0), 237–259,
1173 doi:10.1039/c3fd00042g, 2013.

1174 Schnell, J. L., Naik, V., Horowitz, L. W., Paulot, F., Mao, J., Ginoux, P., Zhao, M. and Ram, K.: Exploring
1175 the relationship between surface PM_{2.5} and meteorology in Northern India, *Atmos. Chem. Phys.*,
1176 18(14), 10157–10175, doi:10.5194/acp-18-10157-2018, 2018.

1177 Sharma, S. K. and Mandal, T. K.: Chemical composition of fine mode particulate matter (PM_{2.5}) in an
1178 urban area of Delhi, India and its source apportionment, *Urban Clim.*, 21, 106–122,
1179 doi:10.1016/j.uclim.2017.05.009, 2017.

1180 Sheesley, R. J., Kirillova, E., Andersson, A., Krusa, M., Praveen, P. S., Budhavant, K., Safai, P. D., Rao,
1181 P. S. P. and Gustafsson, O.: Year-round radiocarbon-based source apportionment of carbonaceous
1182 aerosols at two background sites in South Asia, *J. Geophys. Res. Atmos.*, 117(10),
1183 doi:10.1029/2011JD017161, 2012.

1184 Simon, M., Dada, L., Heinritzi, M., Scholz, W., Stolzenburg, D., Fischer, L., Wagner, A., Kürten, A.,
1185 Rörup, B., He, X.-C., Almeida, J., Baalbaki, R., Baccarini, A., Bauer, P., Beck, L., Bergen, A., Bianchi, F.,
1186 Bräkling, S., Brilke, S., Caudillo, L., Chen, D., Chu, B., Dias, A., Draper, D., Duplissy, J., El Haddad, I.,
1187 Finkenzeller, H., Frege, C., Gonzalez-Carracedo, L., Gordon, H., Granzin, M., Hakala, J., Hofbauer, V.,
1188 Hoyle, C., Kim, C., Kong, W., Lamkaddam, H., Lee, C., Lehtipalo, K., Leiminger, M., Mai, H., Manninen,
1189 H., Marie, G., Marten, R., Mentler, B., Molteni, U., Nichman, L., Nie, W., Ojdanic, A., Onnela, A.,
1190 Partoll, E., Petäjä, T., Pfeifer, J., Philippov, M., Quéléver, L., Ranjithkumar, A., Rissanen, M.,
1191 Schallhart, S., Schobesberger, S., Schuchmann, S., Shen, J., Sipilä, M., Steiner, G., Stozhkov, Y.,
1192 Tauber, C., Tham, Y., Tomé, A., Vazquez-Pufleau, M., Vogel, A., Wagner, R., Wang, M., Wang, D.,
1193 Wang, Y., Weber, S., Wu, Y., Xiao, M., Yan, C., Ye, P., Ye, Q., Zauner-Wieczorek, M., Zhou, X.,
1194 Baltensperger, U., Dommen, J., Flagan, R., Hansel, A., Kulmala, M., Volkamer, R., Winkler, P.,
1195 Worsnop, D., Donahue, N., Kirkby, J. and Curtius, J.: Molecular understanding of new-particle

1196 formation from alpha-pinene between α -pinene and β -pinene and
1197 α -pinene, Atmos. Chem. Phys., (January), 1–42, doi:10.5194/acp-2019-1058,
1198 2020.

1199 Sindelarova, K., Granier, C., Bouarar, I., Guenther, A., Tilmes, S., Stavrou, T., Müller, J. F., Kuhn, U.,
1200 Stefani, P. and Knorr, W.: Global data set of biogenic VOC emissions calculated by the MEGAN model
1201 over the last 30 years, Atmos. Chem. Phys., 14(17), 9317–9341, doi:10.5194/ACP-14-9317-2014,
1202 2014.

1203 Singh, B. P., Kumar, K. and Jain, V. K.: Source identification and health risk assessment associated
1204 with particulate- and gaseous-phase PAHs at residential sites in Delhi, India, Air Qual. Atmos. Heal.,
1205 doi:10.1007/S11869-021-01035-5, 2021.

1206 Singh, D. P., Gadi, R. and Mandal, T. K.: Characterization of Gaseous and Particulate Polycyclic
1207 Aromatic Hydrocarbons in Ambient Air of Delhi, India, Polycycl. Aromat. Compd., 32(4), 556–579,
1208 doi:10.1080/10406638.2012.683230, 2012.

1209 Sinha, V., Kumar, V. and Sarkar, C.: Chemical composition of pre-monsoon air in the Indo-Gangetic
1210 Plain measured using a new air quality facility and PTR-MS: High surface ozone and strong influence
1211 of biomass burning, Atmos. Chem. Phys., 14(12), 5921–5941, doi:10.5194/acp-14-5921-2014, 2014.

1212 Spolnik, G., Wach, P., Rudzinski, K. J., Skotak, K., Danikiewicz, W. and Szmigielski, R.: Improved
1213 UHPLC-MS/MS Methods for Analysis of Isoprene-Derived Organosulfates, Anal. Chem., 90(5), 3416–
1214 3423, doi:10.1021/acs.analchem.7b05060, 2018.

1215 Stewart, G. J., Nelson, B. S., Acton, W. J. F., Vaughan, A. R., Farren, N. J., Hopkins, J. R., Ward, M. W.,
1216 Swift, S. J., Arya, R., Mondal, A., Jangirh, R., Ahlawat, S., Yadav, L., Sharma, S. K., Yunus, S. S. M.,
1217 Hewitt, C. N., Nemitz, E., Mullinger, N., Gadi, R., Sahu, L. K., Tripathi, N., Rickard, A. R., Lee, J. D.,
1218 Mandal, T. K. and Hamilton, J. F.: Emissions of intermediate-volatility and semi-volatile organic
1219 compounds from domestic fuels used in Delhi, India, Atmos. Chem. Phys., 21(4), 2407–2426,
1220 doi:10.5194/ACP-21-2407-2021, 2021a.

1221 Stewart, G. J., Acton, W. J. F., Nelson, B. S., Vaughan, A. R., Hopkins, J. R., Arya, R., Mondal, A.,
1222 Jangirh, R., Ahlawat, S., Yadav, L., Sharma, S. K., Dunmore, R. E., Yunus, S. S. M., Nicholas Hewitt, C.,
1223 Nemitz, E., Mullinger, N., Gadi, R., Sahu, L. K., Tripathi, N., Rickard, A. R., Lee, J. D., Mandal, T. K. and
1224 Hamilton, J. F.: Emissions of non-methane volatile organic compounds from combustion of domestic
1225 fuels in Delhi, India, Atmos. Chem. Phys., 21(4), 2383–2406, doi:10.5194/ACP-21-2383-2021, 2021b.

1226 Stewart, G. J., Nelson, B. S., Drysdale, W. S., Acton, W. J. F., Vaughan, A. R., Hopkins, J. R., Dunmore,
1227 R. E., Hewitt, C. N., Nemitz, E., Mullinger, N., Langford, B., Shivani, Reyes-Villegas, E., Gadi, R.,
1228 Rickard, A. R., Lee, J. D. and Hamilton, J. F.: Sources of non-methane hydrocarbons in surface air in
1229 Delhi, India, Faraday Discuss., 226(0), 409–431, doi:10.1039/D0FD00087F, 2021c.

1230 Surratt, J. D., Murphy, S. M., Kroll, J. H., Ng, N. L., Hildebrandt, L., Sorooshian, A., Szmigielski, R.,
1231 Vermeylen, R., Maenhaut, W., Claeys, M., Flagan, R. C. and Seinfeld, J. H.: Chemical composition of
1232 secondary organic aerosol formed from the photooxidation of isoprene, J. Phys. Chem. A, 110(31),
1233 9665–9690, doi:10.1021/jp061734m, 2006.

1234 Surratt, J. D., Kroll, J. H., Kleindienst, T. E., Edney, E. O., Claeys, M., Sorooshian, A., Ng, N. L.,
1235 Offenberg, J. H., Lewandowski, M., Jaoui, M., Flagan, R. C. and Seinfeld, J. H.: Evidence for
1236 Organosulfates in Secondary Organic Aerosol, Environ. Sci. Technol., 41(2), 517–527,
1237 doi:10.1021/es062081q, 2007.

1238 Surratt, J. D., Gómez-González, Y., Chan, A. W. H., Vermeylen, R., Shahgholi, M., Kleindienst, T. E.,
1239 Edney, E. O., Offenberg, J. H., Lewandowski, M., Jaoui, M., Maenhaut, W., Claeys, M., Flagan, R. C.
1240 and Seinfeld, J. H.: Organosulfate Formation in Biogenic Secondary Organic Aerosol, J. Phys. Chem. A,

1241 112(36), 8345–8378, doi:10.1021/jp802310p, 2008a.

1242 Surratt, J. D., Gómez-González, Y., Chan, A. W. H., Vermeylen, R., Shahgholi, M., Kleindienst, T. E.,
1243 Edney, E. O., Offenberg, J. H., Lewandowski, M., Jaoui, M., Maenhaut, W., Claeys, M., Flagan, R. C.
1244 and Seinfeld, J. H.: Organosulfate Formation in Biogenic Secondary Organic Aerosol, *J. Phys. Chem. A*,
1245 112(36), 8345–8378, doi:10.1021/jp802310p, 2008b.

1246 Surratt, J. D., Chan, A. W. H., Eddingsaas, N. C., Chan, M., Loza, C. L., Kwan, A. J., Hersey, S. P., Flagan,
1247 R. C., Wennberg, P. O. and Seinfeld, J. H.: Reactive intermediates revealed in secondary organic
1248 aerosol formation from isoprene, *Proc. Natl. Acad. Sci.*, 107(15), 6640–6645,
1249 doi:10.1073/pnas.0911114107, 2010.

1250 Szidat, S., Jenk, T. M., Gäggeler, H. W., Synal, H. A., Fisseha, R., Baltensperger, U., Kalberer, M.,
1251 Samburova, V., Wacker, L., Saurer, M., Schwikowski, M. and Hajdas, I.: Source apportionment of
1252 aerosols by ¹⁴C measurements in different carbonaceous particle fractions, in *Radiocarbon*, vol. 46,
1253 pp. 475–484, University of Arizona, 2004.

1254 Takeuchi, M. and Ng, N. L.: Chemical composition and hydrolysis of organic nitrate aerosol formed
1255 from hydroxyl and nitrate radical oxidation of α -pinene and β -pinene, *Atmos. Chem. Phys.*, 19(19),
1256 12749–12766, doi:10.5194/ACP-19-12749-2019, 2019.

1257 Wagner, P. and Kuttler, W.: Biogenic and anthropogenic isoprene in the near-surface urban
1258 atmosphere — A case study in Essen, Germany, *Sci. Total Environ.*, 475, 104–115,
1259 doi:10.1016/J.SCITOTENV.2013.12.026, 2014.

1260 Wang, J. L., Chew, C., Chang, C. Y., Liao, W. C., Lung, S. C. C., Chen, W. N., Lee, P. J., Lin, P. H. and
1261 Chang, C. C.: Biogenic isoprene in subtropical urban settings and implications for air quality, *Atmos.*
1262 *Environ.*, 79, 369–379, doi:10.1016/J.ATMOENV.2013.06.055, 2013.

1263 Wang, X., Hayeck, N., Brüggemann, M., Yao, L., Chen, H., Zhang, C., Emmelin, C., Chen, J., George, C.
1264 and Wang, L.: Chemical Characteristics of Organic Aerosols in Shanghai: A Study by Ultrahigh-
1265 Performance Liquid Chromatography Coupled With Orbitrap Mass Spectrometry, *J. Geophys. Res.*
1266 *Atmos.*, 122(21), 11,703–11,722, doi:10.1002/2017JD026930, 2017.

1267 Wang, X. K., Rossignol, S., Ma, Y., Yao, L., Wang, M. Y., Chen, J. M., George, C. and Wang, L.:
1268 Molecular characterization of atmospheric particulate organosulfates in three megacities at the
1269 middle and lower reaches of the Yangtze River, *Atmos. Chem. Phys.*, 16(4), 2285–2298,
1270 doi:10.5194/acp-16-2285-2016, 2016.

1271 Wang, Y., Hu, M., Guo, S., Wang, Y., Zheng, J., Yang, Y., Zhu, W., Tang, R., Li, X., Liu, Y., Le Breton, M.,
1272 Du, Z., Shang, D., Wu, Y., Wu, Z., Song, Y., Lou, S., Hallquist, M. and Yu, J.: The secondary formation
1273 of organosulfates under interactions between biogenic emissions and anthropogenic pollutants in
1274 summer in Beijing, *Atmos. Chem. Phys.*, 18(14), 10693–10713, doi:10.5194/acp-18-10693-2018,
1275 2018a.

1276 Wang, Y., Hu, M., Guo, S., Wang, Y., Zheng, J., Yang, Y., Zhu, W., Tang, R., Li, X., Liu, Y., Le Breton, M.,
1277 Du, Z., Shang, D., Wu, Y., Wu, Z., Song, Y., Lou, S., Hallquist, M. and Yu, J.: The secondary formation
1278 of organosulfates under interactions between biogenic emissions and anthropogenic pollutants in
1279 summer in Beijing, *Atmos. Chem. Phys.*, 18(14), 10693–10713, doi:10.5194/acp-18-10693-2018,
1280 2018b.

1281 Wang, Y., Tong, R. and Yu, J. Z.: Chemical Synthesis of Multifunctional Air Pollutants: Terpene-
1282 Derived Nitrooxy Organosulfates, *Environ. Sci. Technol.*, acs.est.1c00348,
1283 doi:10.1021/acs.est.1c00348, 2021a.

1284 Wang, Y., Zhao, Y., Wang, Y., Yu, J. Z., Shao, J., Liu, P., Zhu, W., Cheng, Z., Li, Z., Yan, N. and Xiao, H.:

1285 Organosulfates in atmospheric aerosols in Shanghai, China: Seasonal and interannual variability,
1286 origin, and formation mechanisms, *Atmos. Chem. Phys.*, 21(4), 2959–2980, doi:10.5194/acp-21-
1287 2959-2021, 2021b.

1288 Wennberg, P. O., Bates, K. H., Crouse, J. D., Dodson, L. G., McVay, R. C., Mertens, L. A., Nguyen, T.
1289 B., Praske, E., Schwantes, R. H., Smarte, M. D., St Clair, J. M., Teng, A. P., Zhang, X. and Seinfeld, J. H.:
1290 Gas-Phase Reactions of Isoprene and Its Major Oxidation Products, *Chem. Rev.*, 118(7), 3337–3390,
1291 doi:10.1021/acs.chemrev.7b00439, 2018.

1292 WHO: WHO | Ambient air pollution, WHO, 2018.

1293 Wozniak, A. S., Bauer, J. E. and Dickhut, R. M.: Characteristics of water-soluble organic carbon
1294 associated with aerosol particles in the eastern United States, *Atmos. Environ.*, 46, 181–188,
1295 doi:10.1016/j.atmosenv.2011.10.001, 2012.

1296 Xu, J., Song, S., Harrison, R. M., Song, C., Wei, L., Zhang, Q., Sun, Y., Lei, L., Zhang, C., Yao, X., Chen,
1297 D., Li, W., Wu, M., Tian, H., Luo, L., Tong, S., Li, W., Wang, J., Shi, G., Huangfu, Y., Tian, Y., Ge, B., Su,
1298 S., Peng, C., Chen, Y., Yang, F., Mihajlić-Zelić, A., Đorđević, D., Swift, S. J., Andrews, I., Hamilton, J. F.,
1299 Sun, Y., Kramawijaya, A., Han, J., Saksakulkrai, S., Baldo, C., Hou, S., Zheng, F., Daellenbach, K. R.,
1300 Yan, C., Liu, Y., Kulmala, M., Fu, P. and Shi, Z.: An interlaboratory comparison of aerosol inorganic ion
1301 measurements by ion chromatography: Implications for aerosol pH estimate, *Atmos. Meas. Tech.*,
1302 13(11), 6325–6341, doi:10.5194/AMT-13-6325-2020, 2020.

1303 Xu, L., Guo, H., Boyd, C. M., Klein, M., Bougiatioti, A., Cerully, K. M., Hite, J. R., Isaacman-VanWertz,
1304 G., Kreisberg, N. M., Knote, C., Olson, K., Koss, A., Goldstein, A. H., Hering, S. V., Gouw, J. de,
1305 Baumann, K., Lee, S.-H., Nenes, A., Weber, R. J. and Ng, N. L.: Effects of anthropogenic emissions on
1306 aerosol formation from isoprene and monoterpenes in the southeastern United States, *Proc. Natl.
1307 Acad. Sci.*, 112(1), 37–42, doi:10.1073/PNAS.1417609112, 2015.

1308 Yadav, A. K., Sarkar, S., Jyethi, D. S., Rawat, P., Aithani, D., Siddiqui, Z. and Khillare, P. S.: Fine
1309 Particulate Matter Bound Polycyclic Aromatic Hydrocarbons and Carbonaceous Species in Delhi's
1310 Atmosphere: Seasonal Variation, Sources, and Health Risk Assessment, *Aerosol Sci. Eng.* 2021 52,
1311 5(2), 193–213, doi:10.1007/S41810-021-00094-6, 2021.

1312 Yee, L. D., Isaacman-VanWertz, G., Wernis, R. A., Kreisberg, N. M., Glasius, M., Riva, M., Surratt, J. D.,
1313 de Sá, S. S., Martin, S. T., Alexander, M. L., Palm, B. B., Hu, W., Campuzano-Jost, P., Day, D. A.,
1314 Jimenez, J. L., Liu, Y., Misztal, P. K., Artaxo, P., Viegas, J., Manzi, A., de Souza, R. A. F., Edgerton, E. S.,
1315 Baumann, K. and Goldstein, A. H.: Natural and Anthropogenically Influenced Isoprene Oxidation in
1316 Southeastern United States and Central Amazon, *Environ. Sci. Technol.*,
1317 doi:10.1021/acs.est.0c00805, 2020.

1318 Zhang, H., Yee, L. D., Lee, B. H., Curtis, M. P., Worton, D. R., Isaacman-VanWertz, G., Offenberg, J. H.,
1319 Lewandowski, M., Kleindienst, T. E., Beaver, M. R., Holder, A. L., Lonneman, W. A., Docherty, K. S.,
1320 Jaoui, M., Pye, H. O. T., Hu, W., Day, D. A., Campuzano-Jost, P., Jimenez, J. L., Guo, H., Weber, R. J.,
1321 De Gouw, J., Koss, A. R., Edgerton, E. S., Brune, W., Mohr, C., Lopez-Hilfiker, F. D., Lutz, A., Kreisberg,
1322 N. M., Spielman, S. R., Hering, S. V., Wilson, K. R., Thornton, J. A. and Goldstein, A. H.: Monoterpenes
1323 are the largest source of summertime organic aerosol in the southeastern United States, *Proc. Natl.
1324 Acad. Sci. U. S. A.*, 115(9), 2038–2043, doi:10.1073/pnas.1717513115, 2018.

1325 Zhang, H., Zhang, Y., Huang, Z., Acton, W. J. F., Wang, Z., Nemitz, E., Langford, B., Mullinger, N.,
1326 Davison, B., Shi, Z., Liu, D., Song, W., Yang, W., Zeng, J., Wu, Z., Fu, P., Zhang, Q. and Wang, X.:
1327 Vertical profiles of biogenic volatile organic compounds as observed online at a tower in Beijing, *J.
1328 Environ. Sci.*, 95, 33–42, doi:10.1016/J.JES.2020.03.032, 2020.

1329 Zhao, D., Schmitt, S. H., Wang, M., Acir, I. H., Tillmann, R., Tan, Z., Novelli, A., Fuchs, H., Pullinen, I.,
1330 Wegener, R., Rohrer, F., Wildt, J., Kiendler-Scharr, A., Wahner, A. and Mentel, T. F.: Effects of NO_x

1331 and SO₂ on the secondary organic aerosol formation from photooxidation of α -pinene and
1332 limonene, *Atmos. Chem. Phys.*, 18(3), 1611–1628, doi:10.5194/acp-18-1611-2018, 2018.

1333 Zhao, D. F., Kaminski, M., Schlag, P., Fuchs, H., Acir, I. H., Bohn, B., Häseler, R., Kiendler-Scharr, A.,
1334 Rohrer, F., Tillmann, R., Wang, M. J., Wegener, R., Wildt, J., Wahner, A. and Mentel, T. F.: Secondary
1335 organic aerosol formation from hydroxyl radical oxidation and ozonolysis of monoterpenes, *Atmos.*
1336 *Chem. Phys.*, 15(2), 991–1012, doi:10.5194/ACP-15-991-2015, 2015.

1337 Zou, Y., Deng, X. J., Deng, T., Yin, C. Q. and Li, F.: One-year characterization and reactivity of isoprene
1338 and its impact on surface ozone formation at a suburban site in Guangzhou, China, *Atmosphere*
1339 (Basel), 10(4), doi:10.3390/ATMOS10040201, 2019.

1340